USING A LOGISTIC PHENOLOGY MODEL WITH IMPROVED DEGREE-DAY ACCUMULATORS TO FORECAST EMERGENCE OF PEST GRASSHOPPERS

PAUL MICHAEL IRVINE
B. Sc. Mathematics, University of Lethbridge, 2003

A Thesis
Submitted to the School of Graduate Studies
of the University of Lethbridge
in Partial Fulfillment of the
Requirements for the Degree

MASTER OF SCIENCE

Department of Mathematics and Computer Science
University of Lethbridge
LETHBRIDGE, ALBERTA, CANADA

Dedication

This thesis is dedicated first and foremost to my twin nephews, Benny and Alex, whom I love very much and who inspire me to be a better person and help make the world a better place for them to live in. Irvine family motto: ***Sub Sole Sub Umbra Virens***

This thesis is also dedicated to my family, my friends, my love, and all people who have disabilities (mental and physical) that challenge them on a daily basis. This is dedicated also to people who rise up in the face of adversity, and thrive anyways.

This thesis is also dedicated to the memory of Patrick Chan, with whom I worked closely and whom I have many fond memories of. Also this thesis is dedicated to Dr. Jim (Jiping) Liu, who was an excellent mentor, professor, and friend.

Abstract

Many organisms, especially animals like insects, which depend on the environment for body heat, have growth stages and life cycles that are highly dependent on temperature. To better understand and model how insect life history events progress, for example in the emergence and initial growth of the biogeographical research subjects, we must first understand the relationship between temperature, heat accumulation, and subsequent development. The measure of the integration of heat over time, usually referred to as degree-days, is a widely used science-based method of forecasting, that quantifies heat accumulation based on measured ambient temperature. Some popular methods for calculation of degree-days are the traditional sinusoidal method and the average method. The average method uses only the average of the daily maximum and minimum temperature, and has the advantage that it is very easy to use. However, this simplest method can underestimate the amount of degree-day accumulation that is occurring in the environment of interest, and thus has a greater potential to reduce the accuracy of forecasting insect pest emergence. The sinusoidal method was popularized by Allen (1976, [1]), and gives a better approximation to the actual accumulation of degree-days. Both of these degree-day accumulators are independent of typical heating and cooling patterns during a typical day cycle. To address possible non-symmetrical effect, it was deemed prudent to construct degree-day accumulators to take into account phenomena like sunrise, sunset, and solar noon. Consideration of these temporal factors eliminated the assumption that heating and cooling in a typical day during the growth season is symmetric. In some tested cases, these newer degree-day integrators are more accurate than the traditional sinusoidal method, and in all tested cases, these integrators are more accurate than the average method. After developing the newer degree-day accumulators, we chose to investigate use of a logistic phenology model similar to one used by Onsager and Kemp (1986, [54]) when studying grasshopper

development. One reason for studying this model is that it has parameters that are important when considering pest management tactics, such as the required degree-day accumulations needed for insects in immature stages (instars) to be completed, as well as a parameter related to the variability of the grasshopper population. Onsager and Kemp used a nonlinear regression algorithm to find parameters for the model. I constructed a simplex algorithm and studied the effectiveness when searching for parameters for a multi-stage insect population model. While investigating the simplex algorithm, it was found that initial values of parameters for constructing the simplex played a crucial role in obtaining realistic and biologically meaningful parameters from the nonlinear regression. Also, while analyzing this downhill simplex method for finding parameters, it was found there is the potential for the simplex to get trapped in many local minima, and thus produce extraneous or incorrectly fitted parameter estimates, although Onsager and Kemp did not mention this problem.

In tests of my methods of fitting, I used an example of daily weather data from Onefour, AB, with a development threshold of 12 °C and a biofix day of April 1st, as an example. The method could be applied to larger, more extensive datasets that include grasshopper population data on numbers per stage, by date, linked to degree accumulations based on the non-symmetrical method, to determine whether it would offer significant improvement in forecasting accuracy of spring insect pest events, over the long term.

Acknowledgments

I would like to thank my supervisors Dan Johnson and David Kaminski for taking me on as a graduate student. Thank you both for believing in me, even when I had my moments of self doubt. I will be forever grateful for your constant encouragement, patience and optimism. Also I would like to thank you both for taking time to help me put together this thesis by reviewing the many drafts it went through and consistently giving me great advice on matters regarding my research and thesis work.

I would also like to thank the following people:

Dr. John Sheriff- for being a member of my supervisory committee, editing my thesis, and helping me get through my first T.A. position for his statistics course.

Dr. Danny Le Roy- for also being a member of my supervisory committee and his helpful comments regarding the structuring of my thesis, as well as giving me the advice to start my thesis work early.

Dr. Brad Hagen and Bill Peifer- for giving me great advice about life and how to approach various circumstances. Also for helping me to maintain a healthy balance of work and play in my life.

Dr. Scott Irvine and Dr. Angela Irvine- for listening to my complaints about being a graduate student and giving me advice for surviving academia and the challenges brought forth by a graduate degree. Also for giving me two amazing nephews for whom this thesis is dedicated.

The late Patrick Chan- for making my days in the office happy ones and for his constant positive attitude.

Dana Andrei- for helping with printing out stuff when I needed it, and for having someone to chat with in the water sciences building.

Craig Weibe, David Zhang, Brittany Turcotte, and Alexis Kaminski- for helping me

Contents

List of Tables

List of Figures

Chapter 1

Introduction

1.1   Overview

This chapter gives a discussion of the need for numerical models that allow forecasting of the timing of insect activity, and a description of some models that have been used. Some of these are currently being used to predict development rates of insects, or by extension proportions of a population of insects that are in a particular age class. The rationale for choosing the logistic phenology model for predicting the occurrence of peak instars for insect populations is described. The models are then applied to the problem of predicting age class progression in populations of grasshoppers on the Canadian Prairies. This insect was chosen because of the very significant damage that can result from its appearance in a wide range of crops, including recent interest in reducing losses in production of lentils, a high-value crop in Canada with considerable benefits for economics and health.

This thesis has the objective of producing a model that can improve upon forecasting methods of pest insects. Also, this thesis strives to provide insights into using a logistic phenology model when modeling growth of pest insects, especially grasshoppers. By improving upon forecasting methods for pest insects, insecticide usage will be reduced. A reduction in pesticide usage will produce economic and environmental benefits (Smith and Holmes (1977, [71],) Gage *et al.* (1982, [16]), [84]).

According to a May 2008 Statistics Canada report, in the last ten years Canadian farmers have harvested an average of 579,400 hectares of lentils per year with an average yield of 1.51 MT per hectare. This represents an average total production of 710,200 MT of lentils grown per annum, totalling farm cash receipts of nearly 194 million dollars (CDN) [73], [13]. This underscores the economic importance of the thesis objective of improving

upon forecasting methods of pest insects that influence the development of these crops.

1.2   Insect pest activity and timing

Economic losses caused by herbivorous insect pests in agriculture and forestry are generally dependent on the timing of insect pest emergence, and subsequent rates of growth and feeding. Crops have stages that are particularly susceptible to insect attack, and pest control actions to reduce the activities or abundance of insects must also be timed carefully in order to be effective and efficient. This is particularly true for vegetation or crop plants that are susceptible in numerous parts of the cycle of plant growth and development. Lentils are a good example. The young lentils can be severely damaged by grasshopper feeding, and in some cases this may result in a need for reseeding, with losses caused by delayed germination and growth. When the plants begin to mature, grasshoppers may feed on the reproductive tissue that will produce harvestable yield. Olfert and Slinkard (1999, [56]) found that two-striped grasshoppers (*Melanoplus bivitattus*) feeding on flowers and developing pods of lentils in Saskatchewan caused severe losses at very low levels of infestation. Populations of only 2-3 per meter squared (about one-fifth of the density that is typically damaging to other crops) resulted in losses of 23% of the pods and 47% of the flowers and immature pods. Grasshoppers can also degrade the final product by their presence in the harvested crop, when dead insect parts reduce the quality and value [84]. In the case of lentils, anticipating the timing and stage of development of the grasshoppers is crucial to directing control efforts that are effective, and use as little insecticide as possible to reduce the risk to acceptable levels. Previously, the timing of age class and related damage risk associated with grasshoppers have been predicted with various approaches to heat summation (Berry et al.(1995, [3]), Regiert (1968, [65]), Gage et al. (1976, [15]), Mukerji et al. (1976, [50]), Mukerji et al.(1977, [51]), Lockwood and Lockwood (1991, [43]), Lactin and John-

son (1996, [38]), Lactin and Johnson (1996, [39], Lactin and Johnson (1995, [36])). An understanding of insect timing and developmental progression is key to pest management strategies, and therefore refinement of predictive models offers benefits for the economics of pest control, for the environment, and for the quality of the resulting food product. Such predictive tools would benefit many farmers who grow pulse crops, especially farmers in Saskatchewan, since they account for 67 percent of lentils produced globally [17].

Insects are dependent on heat from the external environment to emerge from quiescent stages, and complete their life cycles. Therefore, methods for forecasting insect life history events and related economic losses have relied mainly on weather data for estimates of probable insect body temperature and timing. Temperature-based models have become central to pest management (Randell and Mukerji (1974, [63]), Preuss (1983, [60]),Fisher (1994, [14]), Hilbert (1995, [22]), Lactin and Johnson (1998, [40], [41]), also see Appendix A), particularly in temperate zones, because the methods allow more precise anticipation of the calendar dates and expected magnitude of risk (the probable levels of damage to crops, in terms of losses in quantity and quality). As noted, such refinements in the power of prediction are more environmentally sustainable, because pest managers can reduce insecticide use if they have access to better information on the timing and geography of the appearance of susceptible or damaging insect stages. Information is the keystone of sustainable integrated pest management, and this includes general information on pest life cycles and natural enemies, as well as current information on pest life cycle events, such as emergence and maturation.

Insect survival, growth and development can occur only over a limited temperature range. When insect development times (meaning time required to pass from one stage to the next) are measured at temperature intervals, a "U"-shaped curve of time versus temperature results. This "U"-shaped curve can be seen in Fig. 1.1. If the reciprocals of the development times are plotted as rates versus temperature, the relationship appears as a

curve, shown in Fig 1.3. Empirical and biophysical models describe either the time versus temperature or the rate versus temperature numerical relationship of insect development. The rate versus temperature relationship is widely used in models designed to model and/or predict insect development. The rationale for using the rate versus the temperature relationship to predict insect development times is that the mean daily or total growth rates can be accumulated under fluctuating temperature environments. Once the accumulation of the development rates reaches 1.0, the development of the instar (the name for an insect in a particular immature age class) is complete, and the model can be adapted to predict what portion of the development of the population cohort is complete. For this reason, models of development time versus temperature curves are usually used as descriptive tools; however, they can easily be converted to rate versus temperature models by taking the reciprocal of development times to yield development rates.

Typically, a measure of heat accumulation known as degree-days is used to gauge development rates in pest insects. The concept of degree-days is explained in greater detail in Chapter 2 of this thesis. It is important to have accurate tools to measure the amount of degree-days that are "experienced" by the insect and accumulated as successful physiological activity and development. Accurate tools to measure heat accumulation support better predictions of pest insect development and emergence, and thereby also support more effective and sustainable pest management. If estimates for heat accumulation and subsequently pest emergence are incorrect, even by a few days, for example, it can result in additional and very significant damage to crops, and may enhance future risk as undetected pest infestations increase in density or number of locations.

Prediction of heat accumulation (degree-days) may be imprecise, because of sampling error, for example because of the heterogeneity of the soil and crop environment, or it may be inaccurate, providing false information of early emergence of a pest problem, or providing warning too late. Greater accuracy in predicting degree-days is one aim of the

Figure 1.1: A curve showing the "U" shape that occurs when development time versus temperature is plotted.
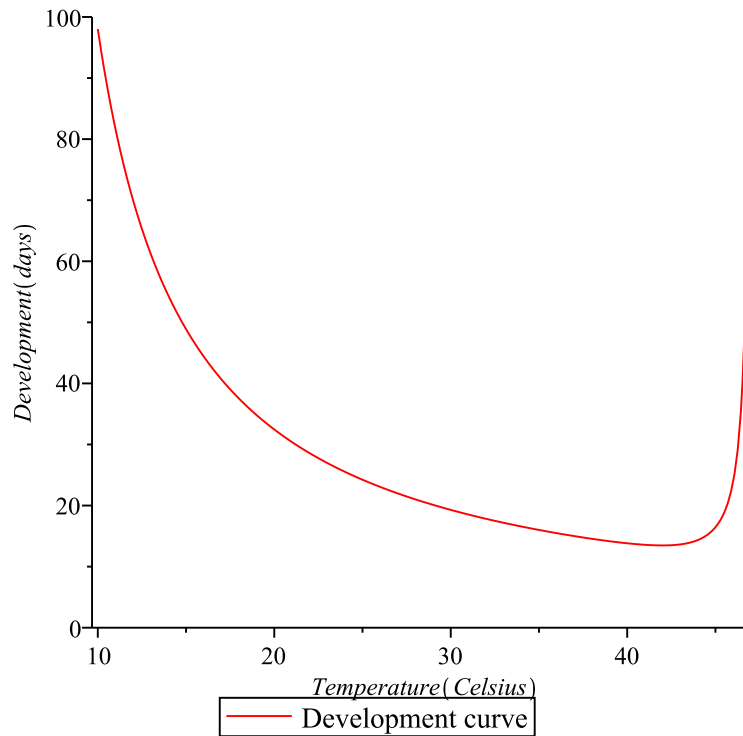
model refinement undertaken in this thesis. With better calculation of degree-days, minimization of financial losses incurred by pest managers can be realized, and inefficient use of pesticide can be prevented. Currently, the "average method", Eqn. (2.1) described in Chapter 2 is widely used as a tool to predict insect emergence, including in Alberta (e.g., Broatch *et al.* (2006, [4]), Eizenberg *et al*, (2005, [11])). Degree-days are used in many places in the US and Canada for pest forecasting and monitoring. For example, in Utah, Table 1.1 and Table 1.2 are supplied so farmers can make their own calculations [80]. On the Canadian Prairies, the Insect Pest Monitoring Network (IPMN, http://www.westernforum.org/IPMNMain.html) uses degree-days as a tool to keep the agriculture industry informed of possible risk to crops due to pest insects. This organization also works with users to conserve natural enemies of these pest species. (A list of example

cases and locations where degree-days are provides and used is listed in appendix A.)

Target Insect	Lower Threshold (°F)	Upper Threshold (°F)
Alfalfa weevil	50	87
Armyworm	50	84
Codling moth	50	88
Peach twig borer	50	88
Peach psylia	41	-

Table 1.1: A partial list of pest insects that occur in Utah and their upper and lower temperature development thresholds.

Target Insect	DD Min	DD Max
Black pineleaf scale	1068	-
Cankerworm	148	290
Lilac root weevil	500	950
Locust borer	2271	2805

Table 1.2: A partial list of degree-day (DD) accumulations for selected landscape pests that occur in Utah. DD Min is the earliest time for appearance and DD Max is the latest time for appearance.

The average method tends to underestimate the amount of degree-days that are actually accumulated. Better or improved degree-day accumulators, coupled with a suitable insect life cycle model, are likely to achieve greater accuracy and precision when predicting grasshopper pest emergence, and therefore support more informed efficient pest management(Johnson (1989, [30]), Logan (1988, [45]), Pannell (1991, [58]), Quinn *et al.* (1993, [62]), Onsager (2000, [55]). tactics.

1.2.1 A brief description of the grasshopper life cycle

During the two weeks following mating, the female grasshopper hunts for an appropriate site to deposit her eggs. Once she selects a site she bores a hole and deposits eggs. She then deposits a foamy secretion over the eggs that hardens them to form an egg pod.

Once the eggs are laid embryological development beings and continues until environmental conditions become unfavourable in the fall and will resume in the spring as the soil temperature rises. Newly hatched grasshoppers, or nymphs, are approximately 5 mm (0.2 of an inch) in length. Nymph are similar in appearance to adults, however nymphs are smaller than adults and also do not have wings.

It will take approximately 35 to 50 days for the nymphs to go through the 5 nymphal or instar (immature grasshopper) stages before becoming a mature grasshopper. Generally the adult females are slightly larger than the males (Johnson (2008, [29]), [18]).

1.3 Insect development models and methods

1.3.1 Earlier rate models

Finding an appropriate model to utilize the improved degree-day accumulators is important to devise optimal pest management strategies. Here I outline some historical models as background for the choice of approach used in this thesis.

Janisch's (1925, 1932, [27, 28]) inverted symmetric and inverted asymmetric catenaries are empirical models [83] used to describe development time as a function of temperature. The catenaries are inverted to give development in units per day. Looking at Eqn. (1.1), the inverted catenary will be symmetric if $b_1 = b_2$; otherwise the function will be asymmetric, as seen in Fig. 1.2. The following equation is the generalized inverted cantenary of Janisch

:

$$\frac{1}{\tau} = \frac{2a}{b_1^{(T-T_m)} + b_2^{(T_m-T)}}. \tag{1.1}$$

Here $\frac{1}{\tau}$ is the development rate at temperature T (in °C). T_m is the temperature where τ is a

Figure 1.2: The solid line represents the situation where $b_1 \neq b_2$ whereas the dashed line shows a symmetric inverted catenary. These curves are plotted with contrived parameters for illustrative purposes and do not relate to any specific insect.
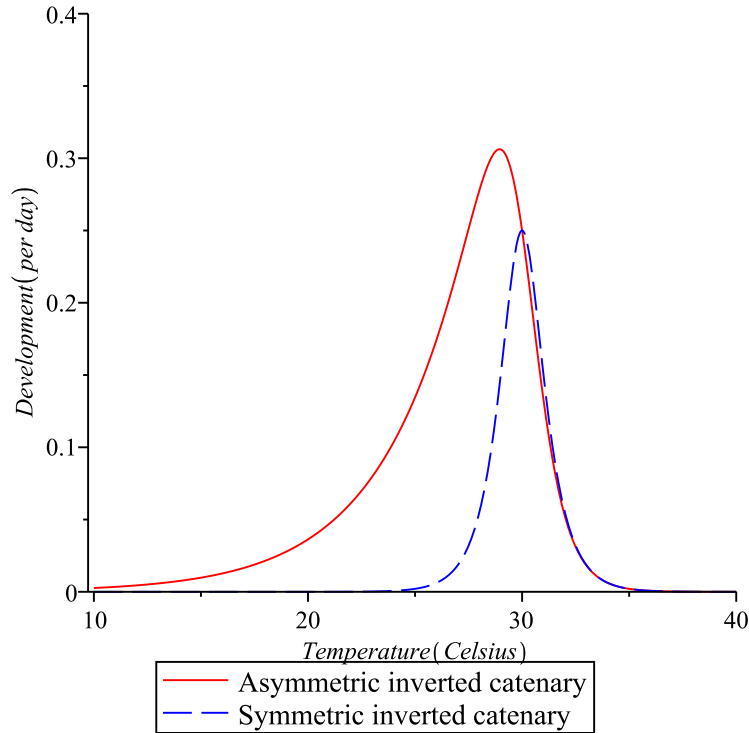
minimum (and development rate is maximal, so in that sense T_m is optimum). Also a is the measured rate at T_m, and b expresses the rate of decline in growth as T diverges from T_m.

Janisch's equation has been used with some degree of success (Rathjen (1939, [64]), Huffaker (1944, [23]), and Quednav (1957, [61])). Some problems associated with it are that it can result in improper fits to data, and can run into computational difficulties (Messenger and Flitters (1958, [48])). The resulting incorrect fitted values can result from bias or from incorrect parameter estimates given by software that calculates the parameters based

on nonlinear regression.

Another equation that describes development rates as a function of temperature is the logistic equation. The logistic equation as used by Davidson (1944, [8]) is

$$\frac{1}{y} = \frac{K}{1 + e^{(a-bx)}},\tag{1.2}$$

where $1/y$ represents the reciprocal of the time required for complete development to be achieved at a given temperature x. K, a and b are constants. Davidson's paper (1942, [7]) does not attribute any biological meaning to these constants.

Davidson (1942, [7]) was one of the first to use a logistic equation to describe insect development rates as a function of temperature. Davidson's treatment with the logistic equation has been widely used (Guppy and Mukerji (1974, [19]), Taylor and Harcourt (1978, [75]), Thomas (1980, [77]), Lamb and Laschiavo (1981, [42])), and Davidson used this logistic equation as early as the 1940s.

1.3.2   More contemporary models

A modified sigmoid equation was used by Stinner *et al.* (1974, [74]) to describe the effects of temperature on insect development rates. The result of Stinner's work led to a development curve similar to that of the logistic equation, however the fitted development rate in Stinner's treatment would drop off after the optimum temperature had been reached [74]. Logan *et al.* (1976, [44]) were able to improve upon Stinner's sigmoid curve by creating a combination of two exponential equations to describe intermediate and high temperature influences on development rates. An additional advantage of Logan's model is that its

parameters have biological meaning. Logan's model equation is:

$$r(T) = \Psi(e^{\rho T} - e^{(\rho T_{max} - \frac{(T_{max} - T)}{\Delta})}).$$ (1.3)

The parameters of Logan's model have the following meanings: Ψ is a directly measurable rate of a temperature-dependent physiological process at some base temperature; ρ can be interpreted as a composite Q_{10}[1] value for critical enzyme-catalyzed biochemical reactions; T_{max} is the thermal maximum (the temperature at which life processes can no longer be sustained except for short durations of time); and Δ is the temperature range at which thermally induced breakdown becomes the overriding factor.

The Logan model cannot estimate a low temperature developmental threshold because the design of the Logan equation will not allow the rate curve to intersect the temperature axis (or the abscissa) at suboptimal temperatures. The low temperature asymptote of the Logan model is 0. Lactin *et al.* (1995, [37]) produced a modified version of the Logan model which eliminates one parameter and introduces another. Their model is exhibited below:

$$r(T) = e^{\rho T} - e^{(\rho T_{max} - \frac{(T_{max} - T)}{\Delta})} + \lambda.$$ (1.4)

The difference between the Lactin and Johnson model and Logan's model is that Ψ is removed and now there is a new parameter, λ, which allows the development curve to intersect the temperature axis at suboptimal temperatures and thus allows estimation of a lower developmental threshold. Thus, this model can take into account intermediate and high temperatures, and also accounts for growth at lower temperatures. A comparison of the Logan model and Lactin and Johnson model can be seen in Fig. (1.3).

---

[1]The temperature coefficient Q_{10} represents the factor by which the rate of a reaction increases for every 10-degree rise in temperature ($^{\circ}$C).

Figure 1.3: A plot comparing the Lactin model with the Logan growth model.
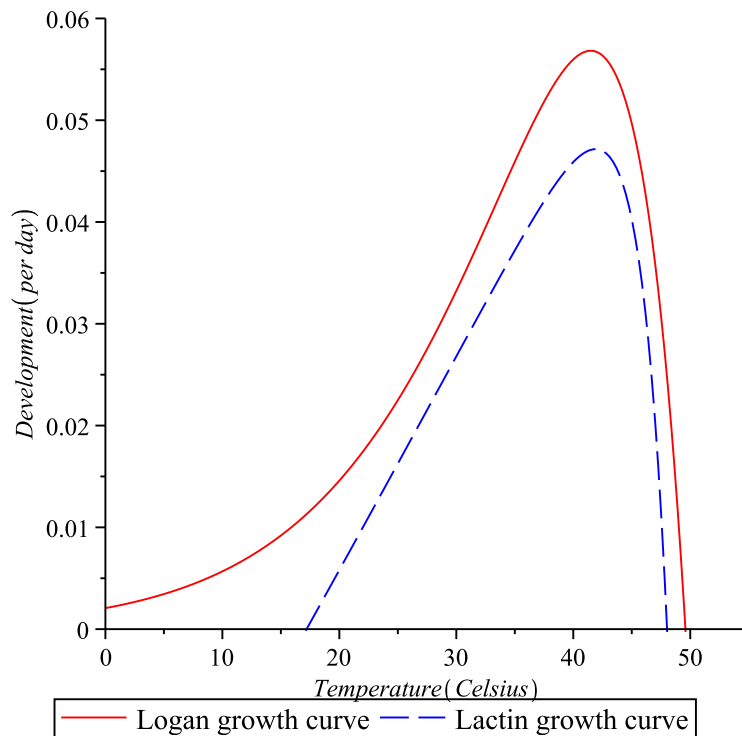
A widely cited growth model was developed by Sharpe and DeMichele (1977, [68]) that describes reaction kinetics of poikilotherm[2] development. Sharpe and DeMichele (1977, [68]) were able to develop a model based on work done by Eyring (1935, [12]), Johnson and Lewis (1946, [31]), and Hultin (1955, [25]). The model that resulted is a complex biophysical model, and has the ability to illustrate nonlinear responses in development rates at both high and low temperatures, along with the standard linear response at intermediate temperatures. The complexity of the model can hinder users who are not familiar with the pitfalls of nonlinear parameter estimation. This makes the model somewhat inaccessible to the general user. Schoolfield *at al.*(1981, [67]) modified the form of the original equation in order to make the model more accessible to the general user. The Schoolfield modification

---

[2]A poikilotherm is a plant or animal whose internal temperature varies along with that of the ambient environmental temperature.

11

to the Sharpe and DeMichele model is listed as follows[3]:

$$A = \frac{RHO25}{298.15} \exp \frac{HA \cdot T - HA \cdot 298.15}{R \cdot 298.15 \cdot T} \tag{1.5}$$

$$B = 1 + \exp \frac{HL \cdot T - HL \cdot TH}{R \cdot TL \cdot T} + \exp \frac{HH \cdot T - HH \cdot TH}{R \cdot TH \cdot T} \tag{1.6}$$

$$r(T) = \frac{A}{B} \tag{1.7}$$

The following list explains the variables of the prior equations:

$r(T)$= the mean development rate (per day) at temperature T (degrees Kelvin);

R= the universal gas constant (8.314472 J K^{-1} mol^{-1});

$RHO25$ = the development rate at 25 degrees Celsius assuming no enzyme activation;

HA= enthalpy of activation of the reaction that is catalyzed by a rate-controlling enzyme;

TL= the temperature at which the rate controlling enzyme is half active and half low temperature inactive;

HL= change in enthalpy associated with low temperature inactivation of the enzyme (in degrees Kelvin);

TH= the temperature at which the rate-controlling enzyme is half active and half high temperature inactive (in degrees Kelvin);

HH= change in the enthalpy associated with the high temperature inactivation of the enzyme.

---

[3]Note that the equations for A and B represent the numerator and denominator for the rate equation, respectively.

Schoolfield's modification of the Sharpe and DeMichele model has six parameters that must be accounted for, and although it seems as though any insect development can be modelled this way, application can be difficult at best for the uninitiated user. The model is best understood with regard to disciplines in temperature-mediated biology.

1.3.3   A stochastic model of insect phenology

Onsager and Kemp (1986, [54]) developed an approach that can be used to predict the proportion of an insect cohort in various developmental stages a function of accumulated degree-days. One assumption of the model is that the development of a particular insect is a stochastic process that consists of an accretion of development times. The process $S(t)$ is defined as the amount of development time that an insect has collected by time t. Degree-day summation is the preferred method by which $S(t)$ and t are measured. The core mechanism of the model is a probability distribution for $S(t)$ that changes as t increases. According to Onsager and Kemp (1986, [54]), the logistic probability density function lent itself well to this model on the basis of accuracy and ease of computations.

For each insect species, the proportion of the population in development stage i at sampling time t is given by the logistic probability density function

$$p_i(t) = Pr[S(t) = i];$$

this in turn gives us the proportion of the population in development stage i at time t, where

the values for $i = 1, \ldots, r$.

$$
\begin{aligned}
p_1(t) &= \left[1 + \exp\left(\frac{-(a_1 - t)}{\sqrt{vt}}\right)\right]^{-1}, \quad i = 1; \\
p_i(t) &= \left[1 + \exp\left(\frac{-(a_i - t)}{\sqrt{vt}}\right)\right]^{-1} - \left[1 + \exp\left(\frac{-(a_{i-1} - t)}{\sqrt{vt}}\right)\right]^{-1}, \quad i = 2, \ldots, r - 1; \\
p_r(t) &= 1 - \left[1 + \exp\left(\frac{-(a_{r-1} - t)}{\sqrt{vt}}\right)\right]^{-1}, \quad i = r,
\end{aligned}
\tag{1.8}
$$

where t is the degree-day accumulation at a particular collection date, a_i is the amount of development needed to complete the ith phenology stage, v is a positive constant, r is the final phenological stage, and $S(t)$ is the amount of development an insect has accumulated at t. This model has attributes that will be discussed further in this thesis since it will be the model that I am primarily working with.

1.4   Choosing a model

After consideration of the attributes of the various models described above, the model that we chose to work with was the stochastic phenology model presented by Onsager and Kemp (1986, [54]). One factor weighing in this decision was the availability of field data as it pertains to instar counts for different geographic locations for different days throughout a particular year, for different years, and for different species [85]. Another reason for this choice is the ease of constructing degree-day integrators to take in large amounts of weather data and calculate degree-day accumulations for various sites for particular days on which grasshopper population data was taken. Grasshopper counts and accumulated degree-days provide enough information to solve for the parameters of the logistic density function proposed by Onager and Kemp (1986, [54]).

The existence of a basis for valid comparison is another reason we chose the stochastic

phenology model. Onsager and Kemp (1986, [54]) calculated parameters for six different species of grasshoppers in the Montana area for years 1975 and 1976. We have additional exemplar data and methodologies for solving the six parameters in the logistic density distribution, for our region and nearby regions. Onsager and Kemp (1986, [54]) use a non-linear optimization technique known as the Nelder-Mead simplex algorithm. This method is used to find the parameters of the stochastic phenology model they propose, and can also be used to fit these parameters to sets of data that are available.

1.5 Thesis outline

This thesis examines the use of a stochastic phenology model as a tool for better predicting the emergence and timing of grasshopper life cycles. Chapter 2 discusses the concept of a degree-day and methodologies used to calculate degree-days. Chapter 3 introduces the setup for finding the parameters of the logistic probability distribution. Chapter 4 discusses the fit and validation of the nonlinear regression that we are applying and some mathematical aspects of our optimization problem. Chapter 5 presents field validation, application, and future work and prospects that can be accomplished with this model.

Chapter 2
Degree-days

2.1 Chapter overview

This chapter looks at some historical methods of calculating degree-days, and explains how some of these methods are imprecise. Also, within this chapter I explain the degree-day accumulation methods that I have developed that take into account temporal aspects of heating and cooling that are occurring within a day. At the end of this chapter there is a comparison of how my accumulators compare with each other, and how they compare to "true degree-day accumulation".

Another aim of this chapter is to familiarize the reader with the concepts of degree-days and accumulated degree-day, since subsequent chapters and their analyses of the logistic phenology model require and understanding of these concepts.

2.2 Physiological time and degree-days

The main component that drives developmental rates of many exothermic organisms is environmental temperature. These temperature-dependent organisms require adequate heat to develop from one point in their life stage to another. Physiological time is the measure of the time passage adjusted for the amount of heat available for the organism to complete life stages. Theoretically, physiological time provides a common reference for the development of organisms. If organisms were completely temperature-dependent, then physiological time would remain a constant for a particular temperature. However, organisms are not completely temperature-dependent, but a large component of their development is based on heat accumulation; thus, estimates for approximate development times can be made.

These approximations of physiological time are often expressed in units called degree-days (Baskerville and Emin (1969, [2]), Higley *et al.* (1986, [21]), [79]).

Figure 2.1: The black area represents the degree-day accumulation. The figure is taken from the site located in the bibliography [79].
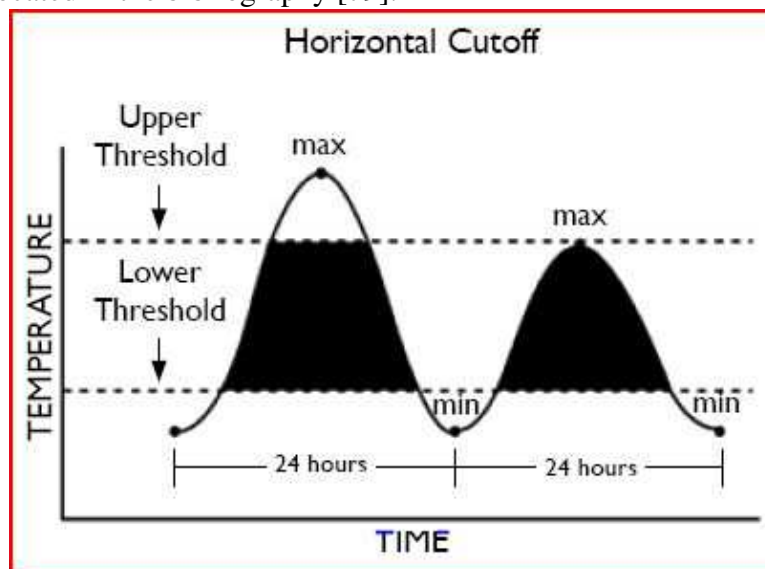
Sometimes called heat units, degree-days are the accumulated product of time and temperature above a particular developmental threshold and below a maximum threshold for an organism. The lower developmental threshold for an organism is the temperature at which development stops. Estimates of upper developmental thresholds also exist for organisms; however, in our treatment of calculating degree-day accumulations for grasshoppers on the Canadian Prairies, these upper thresholds are not met and therefore excluded from our discussion. One degree-day is one day (24 hours) with the temperature one degree above the lower developmental threshold. For example, if our developmental threshold is 12 °C and our temperature remains at 13 °C for 24 hours, then one degree-day is accumulated.

2.3 Methods for calculating degree-days

There are several methods for calculating degree-days. One of the most rudimentary forms for calculating degree-days is done using averages:

$$DD = \max\left(0, \frac{T_{max} + T_{min}}{2} - T_{base}\right).$$ (2.1)

Here DD is the degree-days accumulation for the day, T_{max} is the maximum temperature for that day, T_{min} is the minimum temperature for that day, and T_{base} is the lower developmental threshold. If $\frac{T_{max}+T_{min}}{2} - T_{base}$ is negative, then the accumulation for that particular day is simply set to zero, as a negative accumulation of degree-days would incorrectly imply that growth could be reversed, which is biologically impossible.

This method can have problems with its accuracy of calculating degree-days. It does not take into account the length of heating and cooling periods throughout a day. This method can theoretically overestimate degree-day accumulations when there is a day that has a long period of cool temperatures. For instance, if the temperature is high at the beginning of the day and begins to fall rapidly to a lower temperature that is maintained for the bulk of the day, then degree-days will be overestimated. This method can underestimate degree-day accumulation as well. If there is a particular day where the temperature increases rapidly from a low temperature and maintains a relatively high temperature, the degree day accumulation will be underestimated. In all the cases we tested, this method underestimates the degree-day accumulation.

Depending on the temperature data available, one can use a variety of methods for increasing the precision of calculating degree-days. For example, if a researcher had temperature data recorded every minute, then a rectangular method for calculating degree days would be entirely appropriate. In the rectangular method[1], the recorded temperature minus

---

[1]The rectangular method is just a Riemann sum. In this case, we take the height of the rectangle to be the

the temperature threshold is the height of the rectangle we are using to calculate the degree-days. If the temperature is below the threshold, the area of the rectangle is zero. The length of the rectangle is the amount of time we are measuring this temperature for. In order to get the amount of heat accumulated in degree-days, we need to divide the rectangle by the fraction of a day that the time occupies. In such a case the degree-day accumulation for one minute would be

$$DD = \max\left(0, \frac{T - T_{base}}{1440}\right).$$ (2.2)

Any differences of $T - T_{base}$ that are negative would be set to zero, and the total degree-days accumulated for the particular day would be the sum of the degree-days for the 1440 observations (minutes per day). It is not typical or necessary that a researcher would have 1-minute temperature intervals available for a multitude of locations, so this method is somewhat impractical. More realistically, a researcher would have most major locations with hourly temperature observations, and the rest of the sites with just daily maximum and minimum temperatures available.

Another popular method of calculating degree-days is to fit a sine wave to a particular day. This method was popularized by Allen (1976, [1]) and only requires that a daily temperature maximum and minimum be supplied. From the particular day's maximum and minimum, a sine wave is constructed to fit these two points (see Figs. 2.6 and 2.7). The degree-day accumulation using Allen's modified sine wave is simply the area above the development threshold and the area below the fitted sinusoidal wave. This area can be easily computed by integrating the sine wave and finding the area underneath it, and then subtracting the area below the developmental threshold. This method will be explained in greater detail as it is one of the methods employed in our model for finding degree-day accumulations. This method is widely used (Lysk (2007), [46]).

recorded temperature minus the temperature threshold. Since this measure of height occurs at the start of the rectangle being constructed, we have a left Riemann sum.

Some other methods for finding degree-day accumulation are the linear heating and cooling model (Fig. 2.2), the sinusoidal heating and cooling model (Fig. 2.4), and the sinusoidal heating mixed with the linear cooling model (Fig. 2.6). With these three models we require the the prior day's maximum, the current day's minimum and maximum respectively, and the next day's projected minimum (or recorded minimum if we are using prior data).

2.4 Degree-day accumulators used in the model

The degree-day accumulators that end-users have a choice of utilizing in our constructed model are the traditional sinusoidal method, the linear heating and linear cooling method, the sinusoidal heating and cooling method, and the linear cooling and sinusoidal heating method. The traditional sinusoidal method only requires the maximum and minimum temperatures respectively to estimate the degree-day accumulation for a particular day. The other three accumulators have a temporal aspect that must be accounted for, because they not only require specific temperature information, but also require when these temperatures are occurring.

To capture the temporal aspect of the three time-dependent integrators, a subroutine called SRLOCAT [26] was employed. This subroutine requires the end user to input the particular latitude and longitude for their region of interest. SRLOCAT calculates the sunrise and sunset for a particular day of a year, at that location. The sunrise and sunset give us an idea of how heating and cooling are occurring throughout a day at a specific location. For our purposes, we chose the heating portion of a particular day to begin at sunrise. The beginning of the cooling period is taken as two hours after solar noon [5]. As for solar noon, it was estimated as the midpoint of the time of sunrise and the time of sunset.

2.4.1 Linear heating and cooling

When estimating linear heating and cooling for a particular day, the start of that particular day is taken to be 0:00 hrs and the end of the day is 24:00 hrs. Once the boundaries of time for the day are established, the process for calculating the degree-day accumulation for that day begins. In the program for calculating linear heating and cooling, there are some assumptions to consider: cooling takes place from yesterday's maximum until today's minimum; heating takes place from today's minimum to today's maximum, and cooling takes place from today's maximum to tomorrow's minimum. Given these three asssumptions the degree-day calculation can be split into three sections. The first and the last sections deal with the cooling that takes place during the day, and the second or middle section deals with the heating that takes place for that particular day.

When calculating the degree-day accumulation for the first section (the first cooling section) we have to consider different scenarios. The first and simplest scenario is the temperature profile line falls below the threshold line at the beginning of the day. If this is the case, the degree-day accumulation for that particular portion of the day is zero. The second case occurs when the temperature at the beginning of the day is above the threshold, and the temperature profile cools to a value below the threshold temperature. In this case the degree-day accumulation is

$$DD_1 = \frac{(x_1)(b - T_a)}{48}.$$

(2.3)

In the above equation, DD_1 is the amount of degree-day accumulation, x_1 is where the temperature profile intersects the threshold, b is where the temperature profile intersects the temperature axis at the beginning of the day, and T_a is the temperature below which

Figure 2.2: This is a graph of linear heating and cooling, with the horizontal solid line representing the threshold, and the saw-tooth lines representing the temperature, where the area between the two lines, above the threshold, represents the degree-day accumulation. Here the temperature is measured in °C.
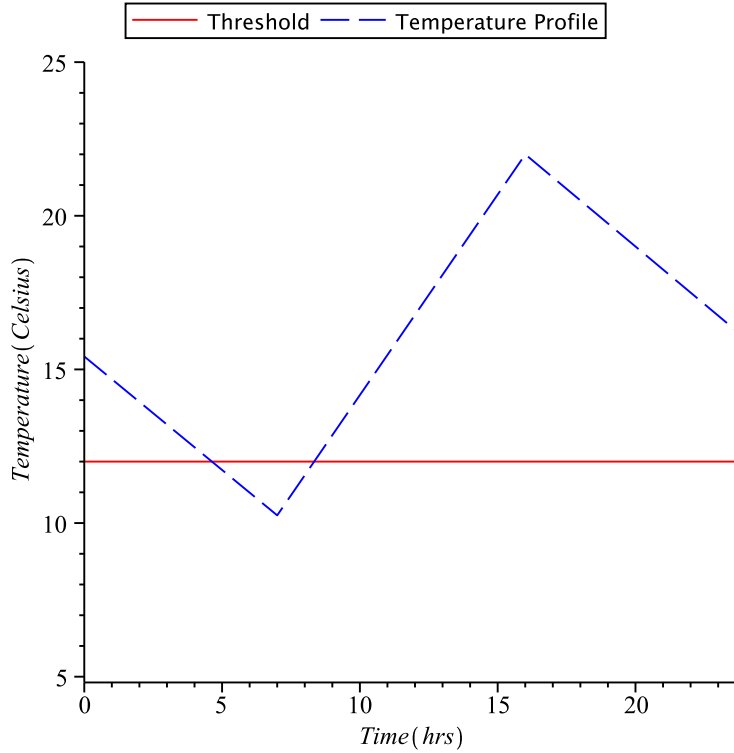
development and accumulation of degree-days stops. Geometrically this calculation is just the area of a triangle. The height of the triangle here is $b - T_a$ and the length of the triangle is x_1. The denominator is set at 48 because it must divided by one half when taking the area of a triangle, and we need to divide by 24 to get the units out of degree-hours and into degree-days.

In the third scenario, the temperature profile crosses the beginning of the day above the temperature threshold and stays above the temperature threshold for the entire cooling period. In this case the degree day accumulation is as follows,

$$DD_1 = \frac{(m_1 - T_a)t_2}{24} + \frac{(t_2)(b - m_1)}{48};$$ (2.4)

22
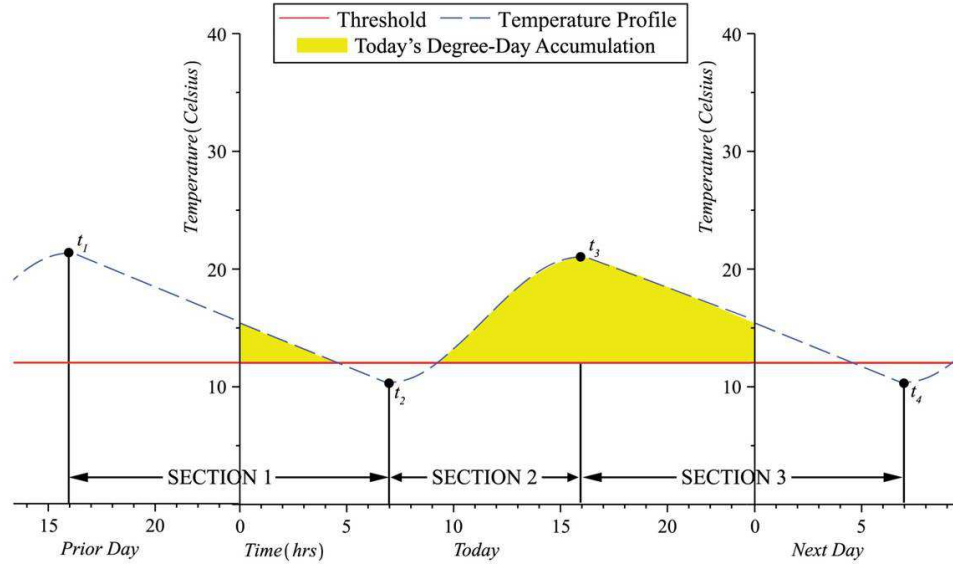
Figure 2.3: An illustration of how the degree-days are calculated with a linear cooling and sinusoidal heating profile. The shaded area represents the degree-day accumulation of the current day (or day of interest). The program we use splits the calculation of degree-days into three sections. The horizontal line at $12\,^{\circ}\text{C}$ represents the development threshold.

where m_1 is the minimum temperature that occurs at time t_2. Also, b, T_a and DD_1 are as previously defined. In this case we have a triangle as before, which has a height of $b - m_1$ and a length of t_2. We also have an additional rectangle that needs to be accounted for and the dimensions of this particular rectangle are $m_1 - T_a$, which is the height of the rectangle, and t_2, the length of the rectangle. Again, in this scenario, we must divide the area of the rectangle by 24 to get out of degree-hour units and into degree-day units.

In the second section of the computation of our degree-days, for one day we are dealing with the temperature profile where heating is occurring. Much like in the first section we have different scenarios. In the first scenario, if the maximum for the particular day is less than the threshold, there will be no degree-day accumulations for either section 2 or 3, because we are under the assumption that the third section of the temperature profile is a cooling section. Thus, if our maximum for this day is lower than our threshold, then the minimum for the next day will also be below the threshold as the temperature profile cools

from today's maximum until tomorrow's minimum. Thus the whole temperature profile for sections 2 and 3 lies below the threshold and therefore no degree-day accumulation occurs.

In another scenario for the second section of the temperature profile, we have today's maximum temperature higher than the threshold, and today's minimum less than the threshold. In this case we have our degree-day accumulation as

$$DD_2 = \frac{(M_2 - T_a)(r_2 - x_2)}{48},$$

(2.5)

where DD_2 is the amount of degree-day accumulation that occurs in the heating section of the day, r_2 is the period of time over which the heating period extends, x_2 is where the temperature profile intersects the threshold line, M_2 is the maximum temperature for the day and T_a is defined as it was previously. Geometrically we are again calculating the area of a triangle where $M_2 - T_a$ is the height of our particular triangle. The length of this triangle is $r_2 - x_2$. We calculate the area of this triangle and divide by 24 to give us our associated degree-days for section two.

In the third scenario, both the daily maximum and minimum temperature lie above the threshold. Here the degree day accumulation for section two is:

$$DD_2 = \frac{r_2(m_1 - T_a)}{24} + \frac{(M_2 - m_1)r_2}{48}.$$

(2.6)

Here all the variables are as previously defined, for the scenario is much like the one encountered in section one, where the degree-day accumulation is equal to the area of a rectangle plus that of a triangle. Here our rectangle has a height of $m_1 - T_a$ and the length of the rectangle is r_2. The triangle has a height of $M_2 - m_1$ and a length of r_2.

In the third section, our temperature profile is in another cooling phase. We have already covered the scenario where no accumulation occurs. One of the other scenarios is where

24

the temperature profile does not intersect the threshold before the end of the day. The degree-day accumulation is

$$DD_3 = \frac{(M_2 - b_1)r_4}{48} + \frac{(b_1 - T_a)r_4}{24},$$ (2.7)

where DD_3 is the accumulation for the third section of the FORTRAN program. Here, r_4 is the amount of time contained in the final cooling period for the day, b_1 is the temperature at the end of the day, and all other variables are as previously defined. r_4 is the length of both the triangle and rectangle, $M_2 - b_1$ is the height of the triangle, and $b_1 - T_a$ is the height of the rectangle. The accumulated degree-days are again the area of the rectangle and triangle.

In the final scenario, our temperature profile crosses the threshold before the day is complete. The associated degree-day accumulation for this final section is computed as

$$DD_3 = \frac{(M_2 - T_a)x_3}{48}.$$ (2.8)

The variables are all defined as before and the only new variable is x_3, which is the time at which the temperature profile crosses the threshold. This equation is just the area of a triangle with height $M_2 - T_a$ and the length x_3. Again the area must be divided by 24 in order to get the proper units of degree-days, and the other factor of 2 in the denominator comes as the result of finding the area of a triangle.

2.4.2 *Sinusoidal heating and cooling*

In this section we explore in detail how the degree-day accumulation works when our temperature profile is simulated by sinusoidal curves, rather than lines, as was the case in the previous subsection of this chapter. In this case, we again have three assumptions about the

heating and cooling sections of a day. Here we assume that the temperatures decrease from yesterday's maximum until today's minimum, and this is the first section of cooling in our day, as well as the first section where degree-day accumulation is computed in our FOR-TRAN program. In the second section, where the day's heating is occurring, we assume that the temperature rises from today's minimum temperature until today's maximum temperature. Finally, in the third section we assume that the temperature profile shows cooling from today's maximum temperature until tomorrow's minimum temperature.

Figure 2.4: This is a graph of sinusoidal heating and cooling, again with the solid line representing the threshold, and the curved dashed line representing the temperature. The degree-day accumulation is as it was represented in Fig. 2.2
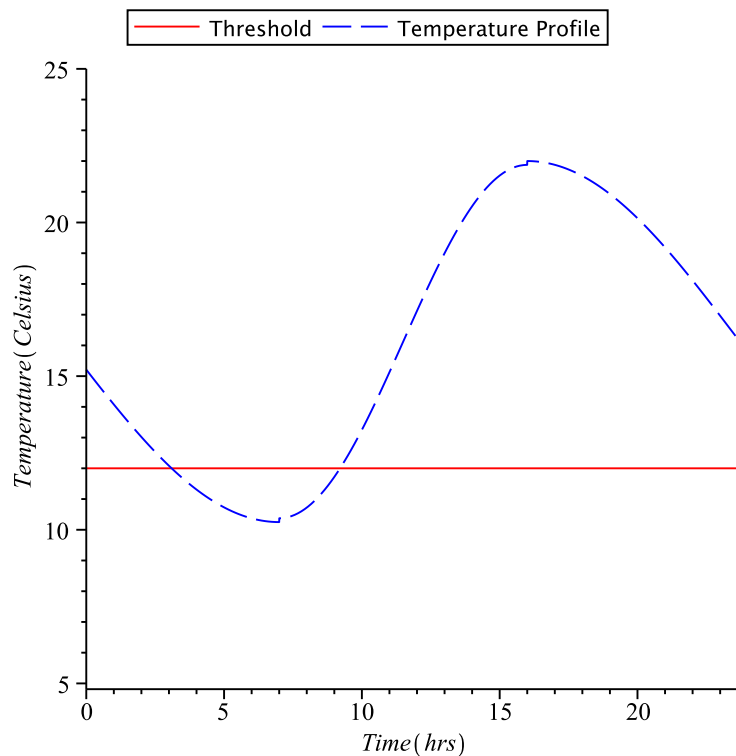
In the first section, if yesterday's maximum temperature is below the threshold, then the degree-day accumulation for the first section is set to zero and the program proceeds. If yesterday's maximum temperature is above the threshold, then we have two possible situations.

26

In the first situation the temperature profile will intersect the threshold before the day's temperature minimum is reached. In this case the degree-day accumulation will be

$$DD_1 = \frac{1}{24} \left(\int_0^{t_1} \left(A \sin \left(\frac{(t+s_1)(2\pi)}{p_1} - \frac{3\pi}{2} \right) + B \right) dt \right) - \frac{T_a \cdot t_1}{24}. \tag{2.9}$$

In this equation the variable t_1 is the time at which the temperature profile intersects the temperature threshold, A is the amplitude of the sine wave, s_1 is the amount of time that elapsed from yesterday's maximum until the beginning of today, p_1 is the period of the sine wave, T_a is the temperature threshold, DD_1 is the amount of degree-day accumulation for this portion of the day, and B is the average of yesterday's maximum temperature and today's minimum temperature. Also note that we are integrating over t (time), hence the differential dt. Also, we are subtracting a rectangular area which is the area below the threshold that is encapsulated by the integral. Notice as well that we are dividing the whole expression by 24 in order to translate the units of degree-hours into degree-days. This is done for Eqs. 2.9 through 2.14.

In the previous scenario, the temperature profile does not intersect the temperature threshold; in this case, the integral is the same as the above with the exception that t_1 is now t_2, the time at which today's minimum occurs. The formula for the degree-day accumulation is as follows:

$$DD_1 = \frac{1}{24} \left(\int_0^{t_2} \left(A \sin \left(\frac{(t+s_1)(2\pi)}{p_1} - \frac{3\pi}{2} \right) + B \right) dt \right) - \frac{T_a \cdot t_2}{24}. \tag{2.10}$$

In sections two and three of the code, we will get zero degree-day accumulation if today's maximum falls below the threshold temperature. This is analogous to the situation that occurred when the temperature profile was modelled by linear heating and cooling. With that knowledge, there are two other scenarios that can occur in section two.

One particular scenario occurs when our temperature profile is initially below the temperature threshold and then crosses the temperature threshold before the day's maximum temperature is reached. In this case, the degree-day accumulation is calculated as

$$DD_2 = \frac{1}{24} \left(\int_{x_2}^{t_3} \left(A_2 \sin \left(\frac{(t - t_2)(2\pi)}{p_2} - \frac{\pi}{2} \right) + B_2 \right) dt \right) - \frac{T_a \cdot (t_3 - x_2)}{24}. \qquad (2.11)$$

The only new variables here are DD_2, which is the degree-day accumulation for the second section of the day. x_2 is the time at which the temperature profile intersects the temperature threshold, t_3 is when today's maximum occurs, A_2 is the amplitude of our sine wave for this particular temperature profile, p_2 is the period of the sine wave for this section of the day, and B_2 is the average of today's minimum and maximum temperatures. Here, t_2 shifts the profile in order to have the sine wave in the proper position. Again we are integrating with respect to t, which represents time.

In the other scenario for section two, we can have the temperature profile completely above the temperature threshold, which changes the limits of integration, and subsequently changes how we calculate the degree-day accumulations for this section of the day. The integral for this case is:

$$DD_2 = \frac{1}{24} \left(\int_{t_2}^{t_3} \left(A_2 \sin \left(\frac{(t - t_2)(2\pi)}{p_2} - \frac{\pi}{2} \right) + B_2 \right) dt \right) - \frac{T_a \cdot (t_3 - t_2)}{24}. \qquad (2.12)$$

The only change from the prior equation is the lower limit of the integral is now t_2 rather than x_2.

In the final section for the day, we again have two scenarios other than the scenario where there is no degree-day accumulation. If the temperature profile does not cross the

28

threshold by the end of the day, our calculation for degree-days is:

$$DD_3 = \frac{1}{24} \left(\int_{t_3}^{24} \left(A_3 \sin\left(\frac{(t-t_3)(2\pi)}{p_3} + \frac{\pi}{2} \right) + B_3 \right) dt \right) - \frac{T_a \cdot (24 - t_3)}{24}. \qquad (2.13)$$

The variable DD_3 is the amount of degree-day accumulation for this section of the day, A_3 is the amplitude of the sine wave for this portion of the temperature profile, B_3 is the average of today's maximum with tomorrow's minimum, p_3 is the period of the sine wave constructed for this portion of the day, and t_3 is the time at which today's maximum occurs and is also the amount the sine wave is shifted in order for it to be in its proper location. The upper limit of the integral is 24, which is the amount of time accumulated at the end of the day in hours. Notice here the rectangular region which we are subtracting has a length of $24 - t_3$ and a height of T_a.

The final scenario for the final section is when the temperature profile intersects the temperature threshold before the end of the day. The only difference between this calculation for degree-days and the other scenario in this final section is that the the upper limit of the integration is x_3, the time at which the temperature profile intersects the temperature threshold. The corresponding calculation for the accumulated degree-days for this section is:

$$DD_3 = \frac{1}{24} \left(\int_{t_3}^{x_3} \left(A_3 \sin\left(\frac{(t-t_3)(2\pi)}{p_3} + \frac{\pi}{2} \right) + B_3 \right) dt \right) - \frac{T_a \cdot (x_3 - t_3)}{24}. \qquad (2.14)$$
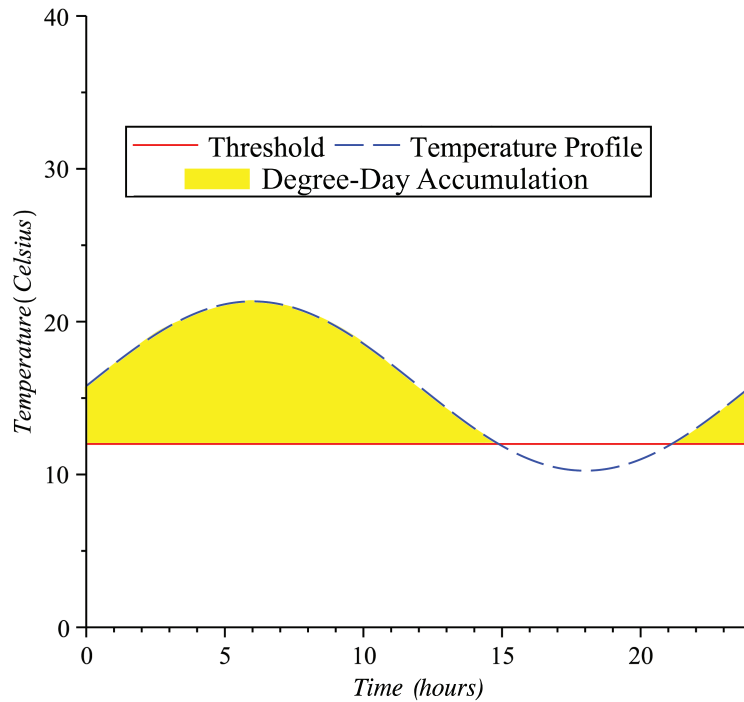
Figure 2.5: An illustration of degree-day accumulation with a traditional sinusoidal heating and cooling profile. The straight line above the time axis represents the temperature development threshold. The shaded area under the sinusoidal curve and above the threshold represents the degree-day accumulation.

2.4.3   Sinusoidal heating and linear cooling

In the sinusoidal heating and linear cooling model of daily temperature, we have a mixture of the all-linear temperature profile and the all-sinusoidal temperature profile. This method is basically a cut-and-paste version of the other two methods. Sections 1 and 3 of the linear cooling are exactly the same as those used in the linear heating and cooling subroutine for finding degree-day accumulations. Also in section 2 of the subroutine, the methodology for finding the accumulated degree-days is exactly the same as in section 2 of the purely sinusoidal temperature profile model. Thus the details are exactly as those found above and therefore omitted from discussion. Figure 2.4 shows what the temperature profile would

look like for a sinusoidal heating and linear cooling model.

Figure 2.6: This figure shows the mixture with sinusoidal heating and linear cooling; the representation of the dashed lines and degree-day accumulations are the same as those in Figs. 2.2 and 2.4.
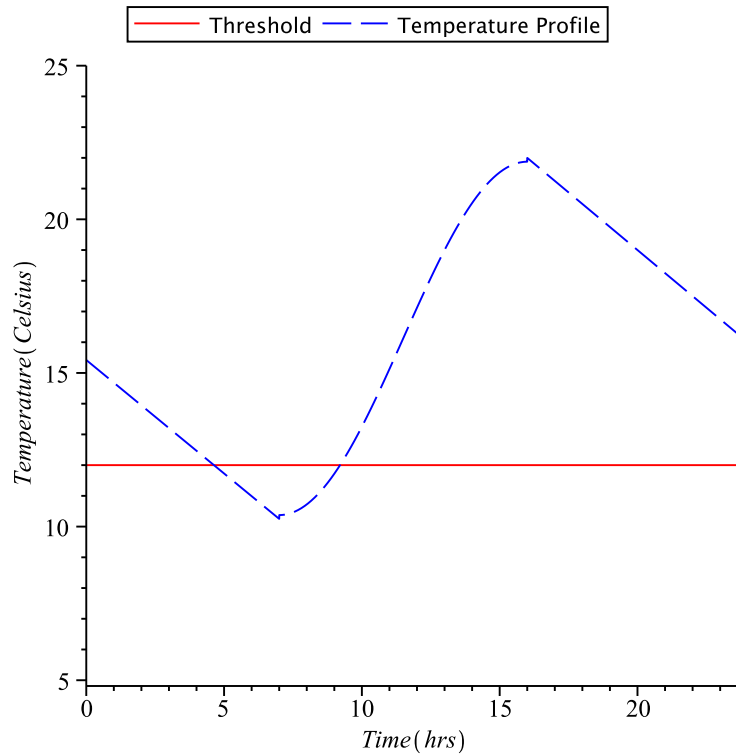
2.4.4 Traditional sinusoidal method

In this model of the temperature profile, there is no temporal dependence, so all that is required is the maximum temperature and the minimum temperature of the day in order to construct the sinusoidal wave.

In this case the calculations for the degree-day accumulations are fairly straightforward. There are four cases that can occur when calculating the degree-day accumulation. The first case is where the maximum for the day is less than the temperature threshold, in which case the degree-day accumulation for the day is zero. Another case is where the whole sine wave

is above the threshold, and the degree day accumulation in this case is:

$$DD_1 = \int_0^1 (A\sin(2\pi t) + B)dt - T_a. \tag{2.15}$$

Here A is the amplitude of the sine wave, B is the average of the minimum and maximum of the sine wave, and T_a is the temperature threshold at which growth stops. Notice that in this case there is no denominator as in other cases, because the units here are already in degree-days whereas in other subroutines the accumulations were in degree-hours based on the temporal variation taken into account.

Another case that occurs can be viewed in Fig. 2.7, where the minimum temperature falls below the threshold during the day, but does so after the start of the day. The degree-day accumulation is as below:

$$DD_1 = \int_0^{t_1} (A\sin(2\pi t) + B)dt + \int_{t_2}^1 (A\sin(2\pi t) + B)dt - T_a \cdot t_1 - T_a \cdot (1 - t_2). \tag{2.16}$$

All the variables are the same as in Eqn. (2.15) and the new variables are t_1 and t_2. Here, t_1 is where the temperature profile crosses the threshold the first time; subsequently, t_2 is where the profile crosses the threshold the second time.

The final method for calculating the degree-day accumulation for the traditional sinusoidal wave occurs when we get a temperature profile as in Fig. 2.8. The integration for the degree day accumulation is

$$DD_1 = 2\int_{t_1}^{\frac{1}{4}} (A\sin(2\pi t) + B)dt - 2T_a \cdot (\frac{1}{4} - t_1). \tag{2.17}$$

In this case, we use the fact that the sinusoidal wave is symmetric around its peak, which occurs at $\frac{1}{4}$ day, or $\frac{\pi}{2}$ days if the day has the length of 2π. In order to get the degree-day accumulation, we integrate from when the temperature profile first crosses the threshold

(t_1) to where the maximum of the sine wave occurs ($\frac{1}{4}$), and multiply the whole integral by two in order to capture all of the area under the curve. In order to remove the area caught by the integral that is below the threshold, we must subtract $2T_a \cdot (\frac{1}{4} - t_1)$, which is the area of rectangle.

Figure 2.7: This figure represents traditional sinusoidal heating and cooling when only the minimum and maximum are used to construct the sine wave; this figure represents the situation where the sine wave is above the threshold at the beginning of the day.
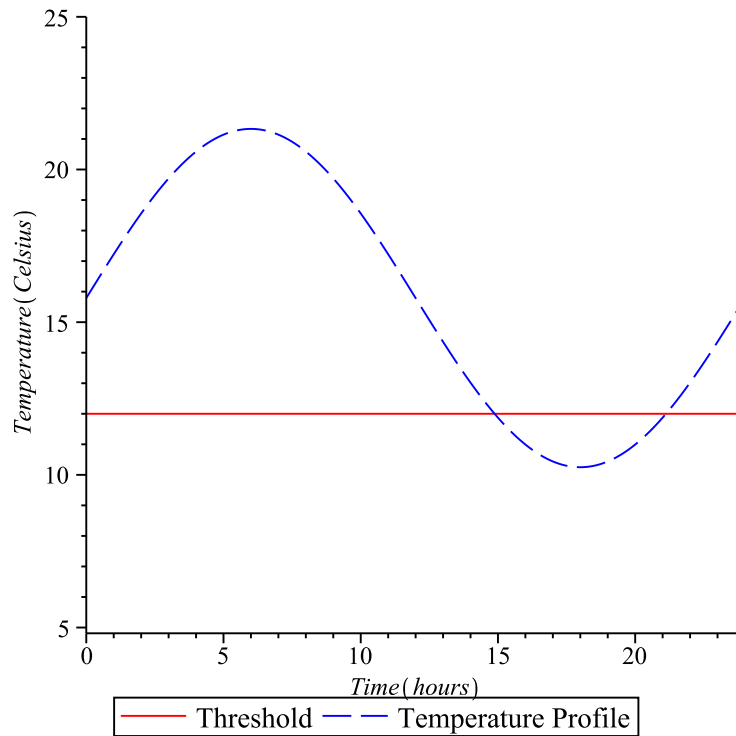
Figure 2.8: This is the same as Fig. 2.7 with the exception that the sine wave is below the threshold when the day begins
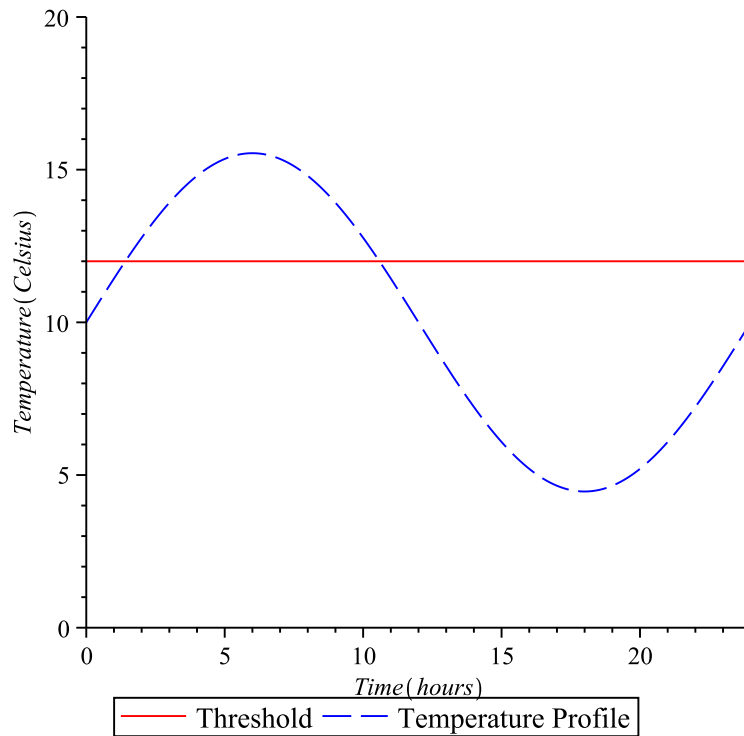
2.5 Comparison of accumulators

For the month of October and up to and including November 6th, 2008, temperatures were recorded at the University of Lethbridge. One of the temperature recording devices was positioned in the soil at a depth of 5cm. The other temperature recording device was positioned 10cm above the ground. Both devices recorded temperature in 10-minute intervals. Such short intervals of measurement allowed observation of temperature fluctuation at this specific time of year, and also allowed us to calculate degree-days with a better precision as discussed earlier in this chapter.

Turning attention to Fig. 2.9, the plot linheat is the degree-day accumulation for the

linear heating and linear cooling accumulator, linsin is the degree-day accumulation for the sinusoidal heating and linear cooling model, sineheat is accumulations produced by sinusoidal heating and cooling that has a temporal dependence, and the traditional sine fit is the accumulator that models temperature based purely on the maximum and minimum temperatures for a day. As a general rule, the linear heating and cooling method always has the lowest accumulation, followed by the mixture of linear heating and cooling, whereas the traditional sinusoidal fit and sineheat have the highest degree-day accumulations and are very close in the values that they produce for the total degree-day accumulations.

To test the general rule above, heat accumulation was tracked at Onefour for the year 2000. The temperature was measured at 2 meters above the ground, as is consistent with most Canadian weather stations. The degree-day accumulation estimated by each accumulator is listed in the table below. These values are tested against a rectangular method of calculating degree-days for each hour, since hourly weather data was available for the Onefour site. The subsequent relative error was then calculated for each degree-day accumulator compared to the rectangular accumulation method. The rectangular method was used as basis for the measured accumulation or "true degree-days." Tables for the University of Lethbridge sites and the Onefour site are below.

air 10 cm	Degree-days (°C)	relative error (percent)
measured accumulation	39.24	-
linheat	35.17	−10.36
sineheat	41.24	5.1
linsin	37.55	−4.30
traditional fit sine wave	40.25	2.57

Table 2.1: Degree-day accumulations at the University of Lethbridge, at a height of 10cm, in the autumn of 2008.

soil 5 cm	Degree-days (°C)	relative error (percent)
measured accumulation	14.42	−
linheat	15.34	6.09
sineheat	17.228	19.47
linsin	16.4497	14.08
traditional fit sine wave	17.561	21.78

Table 2.2: Degree-day accumulations at the University of Lethbridge at a depth of 5cm, in the autumn of 2008.

Air 2 m	Degree-days (°C)	relative error (percent)
measured accumulation	912.65	−
linheat	889.29	−2.56
sineheat	957.18	4.88
linsin	909.40	−0.36
traditional fit sine wave	967.67	6.02

Table 2.3: Degree-day accumulation at the Onefour weather station for the year 2000.

The relative error of the accumulators is much lower in general for the Onefour data sets than those taken at the University of Lethbridge. One reason for the lower relative error in the Onefour data set is that every day during that year was sampled, and therefore we had a relatively large denominator when comparing relative errors as opposed to having smaller denominators for relative error in the University of Lethbridge sample data. Also, with more sampling points for the Onefour data, extreme fluctuations in accumulation or non-accumulation ought to average out, giving a smaller variance of relative errors for the larger data set. The relative error can also be a function of the time of the year at which we were observing the degree-day accumulations. Over the summer months, Onefour would have long periods of stable weather. October, by contrast, can have large fluctuations in degree-day accumulation as the temperature profiles are transitioning from summer to winter.

The range of the relative errors for the Onefour data is from -2.56 percent to 6.02 percent; therefore any degree-day accumulator chosen in the model should give a good approximation of the heat accumulation that is occurring in a specific region. As more information about grasshopper locations becomes available, the model will be adjustable by the end users' requirements for heat accumulation. For example, a user of the model may wish to use linear heating and cooling, because it may better model what is going on in a certain type of soil or terrain. Also, users of the program may opt to go with the sinusoidal heating and cooling model degree-day accumulator or the traditional sinusoidal accumulator. Both of these accumulators tend to overestimate the degree-day accumulation, but this can be beneficial in some scenarios, such as in cases where a particular grasshopper species is able to bask, and thereby increase the amount of heat they are accumulating.

Figure 2.9: Comparison of degree-day accumulation and estimates for temperatures recorded 10 cm above the ground.
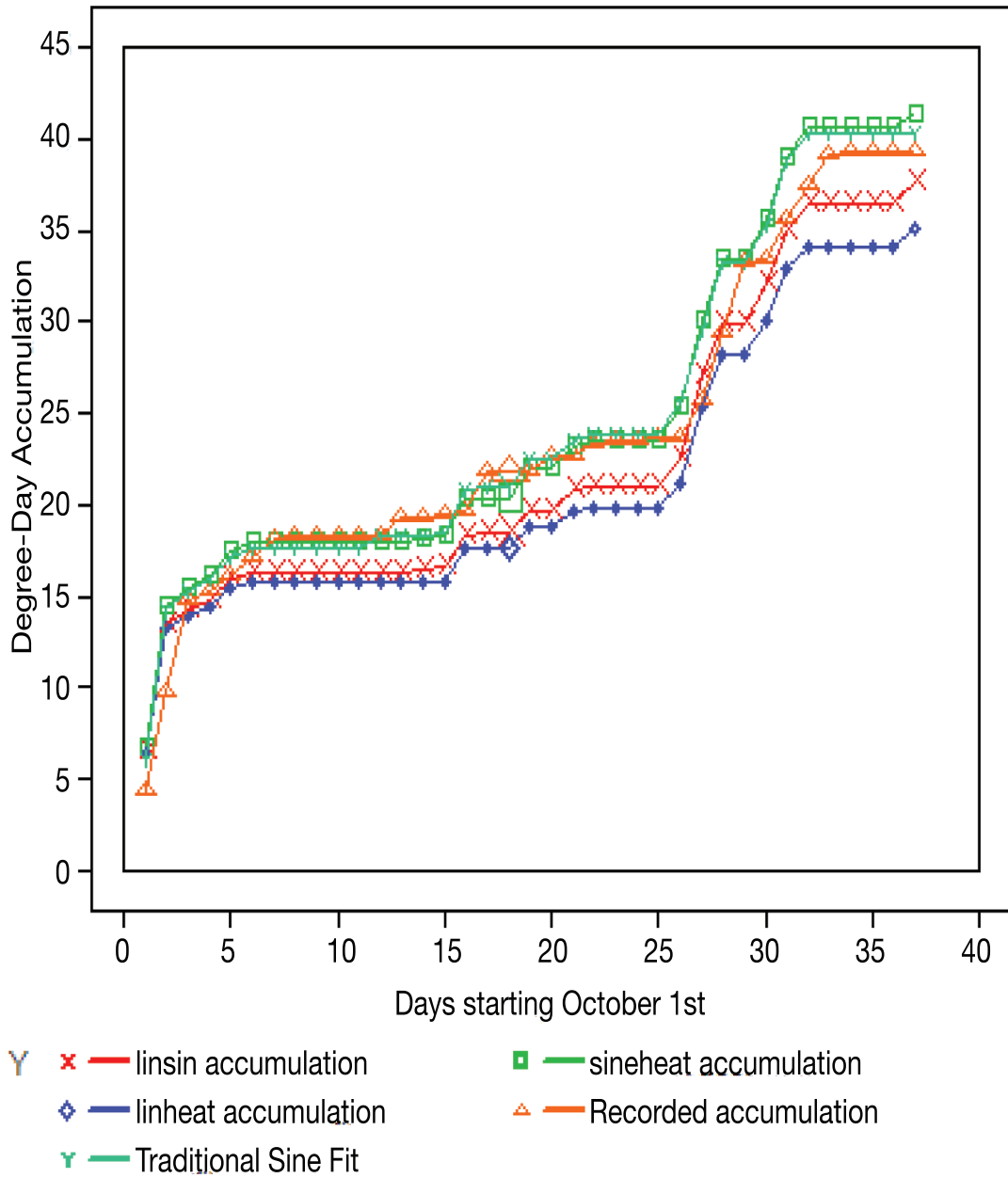
Chapter 3

Model traits and considerations

3.1 Chapter overview

One of the aims of this chapter is to familiarize the reader with how Eqn. (1.8) was developed. Also this chapter investigates various manipulations of parameters in Eqn. (1.8) and how those manipulations effect the logistic phenology model. The constraints for the model are also outlined in this chapter, as the constraints of this model are an important factor in determining initial values for our minimization algorithm (Chapter 4).

3.2 The logistic equation

A logistic equation or logistic curve is a sigmoid curve, thus named by Pierre Verhulst. Verhulst studied the logistic function in its relation to population growth (1838, [81]). Supposing that we had some population P, Verhulst argues that the growth of the population may be modelled by a logistic curve, which has an "S" shape. The initial growth of the population is approximately exponential, then, as the population becomes saturated, growth slows, and eventually the population reaches an upper limit known as the population's carrying capacity. A simplified version of a logistic equation would be

$$P(x) = \frac{1}{1 + \exp(-x)}. \tag{3.1}$$

In this equation P is the population and x is time. As $x \to -\infty$ then $P \to 0$, also as $x \to +\infty$ then $P \to 1$, or increases to the carrying capacity.

The simplified logistic equation used here is what most mathematicians associate with

Figure 3.1: A plot of a simple version of the logistic equation.
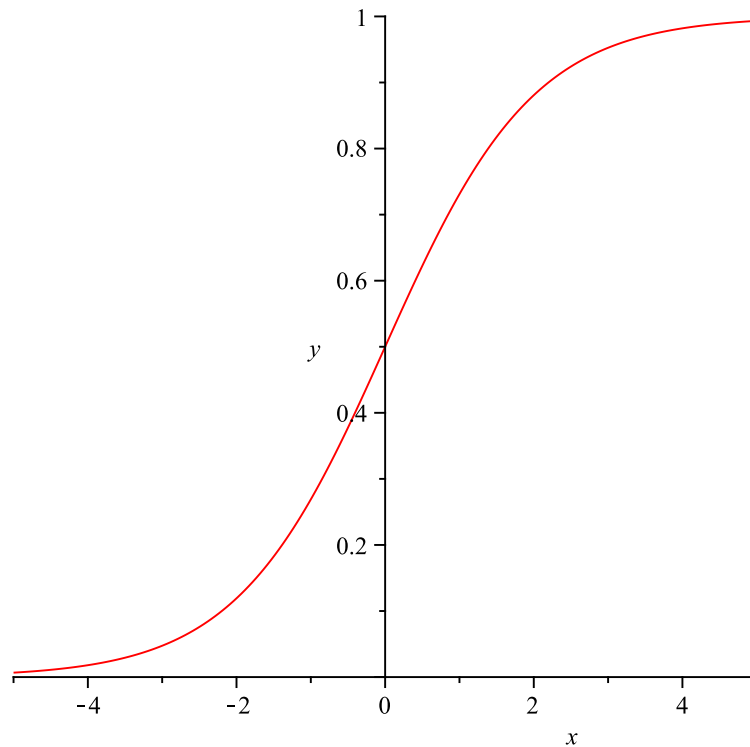
the logistic equation. However, there are variants of the logistic equation or logistic function available. For example, when considering Eqn. (1.8) from the first chapter, the authors who used this model referred to these sets of equations as logistic equations or logistic curves.

Another example of a logistic equation is the "generalized logistic function," and is sometimes known as Richards' curve (Richards (1959, [66])). Richard's curve is an extension of the logistic curve and is also a sigmoid function used in modelling growth:

$$y(t) = A + \frac{K - A}{\left[1 + Q\exp\left(-B(t - M)\right)\right]^{1/\nu}}. \tag{3.2}$$

The variable y can measure weight, height, population, etc. This function has six parameters: A is the lower asymptote; K is the upper asymptote and the carrying capacity if $A = 0$;

B is the growth rate; $v > 0$ affects where maximum growth occurs, Q depends on the value of $y(t_0) = y_0$, where $Q = -1 + \left(\frac{K}{y_0}\right)^v$; and M is the time of maximum growth if $Q = v$. As an illustration, a plot of Richard's curve is given in Fig. 3.2 where $A = 0$, $K = 1$, $B = 1$, $Q = v = 0.5$, $M = 0.5$. As can be seen in Figs. 3.1 and 3.2, the plot of Richard's curve is similar to the plot of the simple logistic equation.

Figure 3.2: A plot of a Richard's equation, or the generalized logistic function.
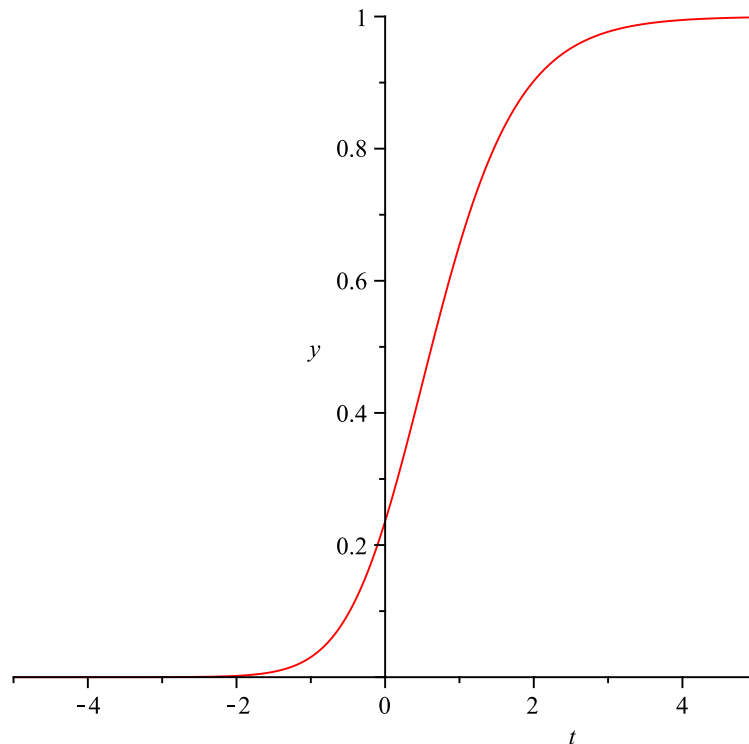
3.2.1   More traits of the logistic equation

When considering the logistic equation in Eq. (3.1), the equation is augmented to have a form of:

$$P(x) = \frac{1}{1 + \exp(x)}. \tag{3.3}$$

Changing the sign of the *x* alters the the logistic curve quite substantially. The curve for this equation is the same as the curve for Eq. (3.1), however, the curve is reflected in the y-axis. This is shown in Fig. 3.3.

Figure 3.3: Comparison of two different forms of the logistic equation.
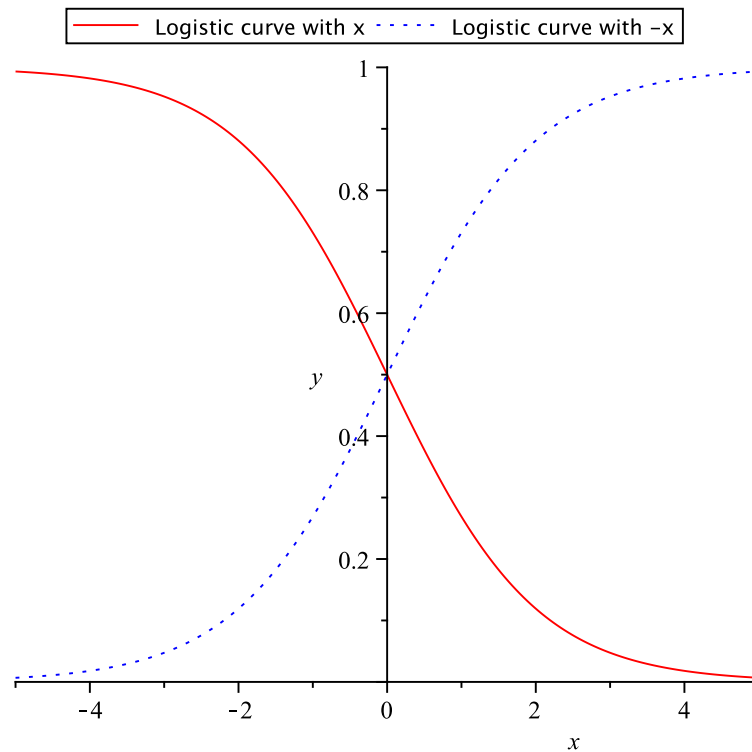
One of the reasons that Eq. (3.3) may be useful is that it is decaying. In biological modelling, this can be useful in showing a population drop to an extinction over time. It is also useful when modelling seasonal insects, as in our case. Seasonal insects have a life stage in which they begin and graduate to successive life stages. This graduation from their beginning life stage to the next life stage is captured when the logistic equation is similar to Eq. (3.3).

When considering the first part of Eq. (1.8), we do have a logistic equation similar in form to Eq. (3.3). The first part of Eq. (1.8) does produce a curve where all of the grasshoppers are in the initial life stage and then move along to the next life stage. A plot

42

of the initial life stage $p_1(t)$ is contained in the first figure of the next section of this chapter, along with plots of the intermediate and final life stages of the grasshopper.

3.2.2 *Taking a difference of logistic equations*

The intermediate life stages reflected in Eq. (1.8) are a difference of logistic equations. Therefore, an examination of the curves produced by logistic equations and their differences seems prudent at this time. First let us consider the following equations:

$$
\begin{aligned}
g(x) &= \frac{1}{1+\exp(-(x-10))}; \\
h(x) &= \frac{1}{1+\exp(-(x-15))}.
\end{aligned}
\tag{3.4}
$$

For a basis of comparison to our model, the equations should be manipulated so that we have $10-x$ and $15-x$ in the equations above giving us $G(x)$ and $H(x)$ rather than the above form:

$$
\begin{aligned}
G(x) &= \frac{1}{1+\exp(-(10-x))}; \\
H(x) &= \frac{1}{1+\exp(-(15-x))}.
\end{aligned}
\tag{3.5}
$$

Plotting these two equations gives us Fig. 3.4. In Fig. 3.4 we can see that the value of $H(x) \geq G(x), \forall\, x$. Also note that the curve for $H(x)$ is translated farther to the right than $G(x)$ in Fig. 3.4. With the use of inequalities we can show that $H(x) \geq G(x), \forall\, x$. If we let $a = 15$ and $b = 10$, we can show that $\forall\, a,b,x$ with $a > b > 0$ and $x > 0$. It follows that

$H(x) \geq G(x), \forall x$. The set of inequalities below gives the desired result:

$$
\begin{aligned}
a &> b \\
\exp(-(a-x)) &> \exp(-(b-x)) \\
\frac{1}{1+\exp(-(a-x))} &> \frac{1}{1+\exp(-(b-x))}
\end{aligned}
$$

In Fig. 3.5, we have a plot of $G(x)$, $H(x)$, and their difference, $I(x)$.

$$
I(x) = \frac{1}{1+\exp(-(15-x))} - \frac{1}{1+\exp(-(10-x))} \tag{3.6}
$$

The difference of the two logistic equations yields a curve that starts off at zero, rises to a definite peak and then again decreases to zero. The shape of this curve is the same as the shape of the intermediate stages of the logistic probability model, and can be compared to Fig. 3.8 in §3.2. This type of curve is useful in modelling insects in that the insect population that has already been through its first life stage will begin to increase in successive life stages, reach a peak for the percentage of the insect populations in that stage, and then decline as the insect population moves on to later development stages.

Figure 3.4: Comparison of two logistic equations with different translations in regards to the *x*-axis. These are the set of equations in Eq. (3.5).
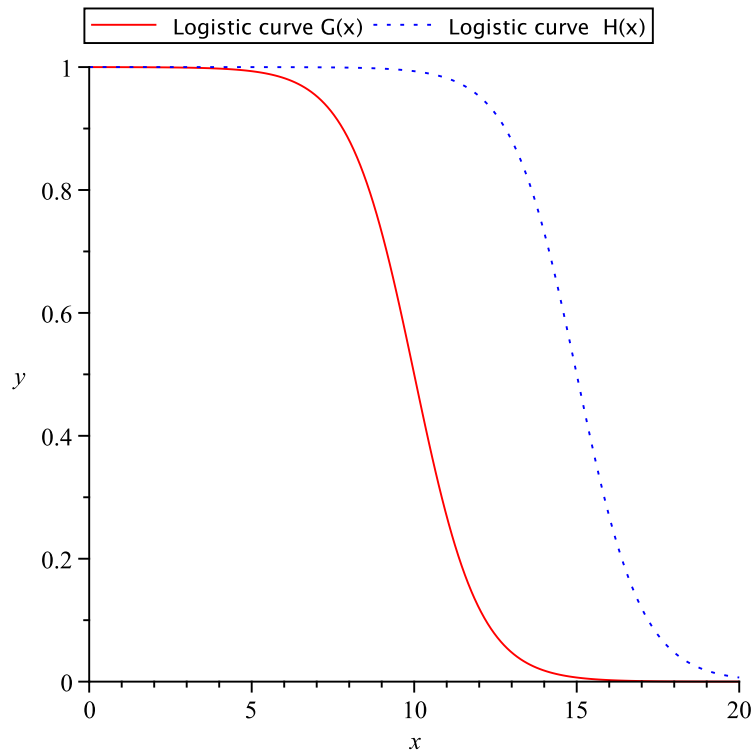
Another form of the logistic equation we want to consider is one similar to that of the final stage of insect development in Eq. (1.8). In this case we would obtain a logistic curve of the form:

$$P(x) = 1 - \frac{1}{1 + \exp\left(-(15 - x)\right)} \tag{3.7}$$

Fig. 3.6 illustrates this curve. Here, as our time variable, *x*, moves ahead, the amount of insects in the population at this stage begin to increase until all insects in the population reach this final life stage. In this case *y* is the proportion of the population in the final life stage and eventually all the insects in the population graduate to this final life stage within a certain time frame. This is similar to what happens in general for seasonal insects: by the time the growth season is nearing its end for insects, the particular insect population is comprised of the adult form of those insects [24]. As shown, the logistic curve of Fig. 3.6

45

Figure 3.5: The plot of $G(x)$, $H(x)$ and their difference, $I(x)$.
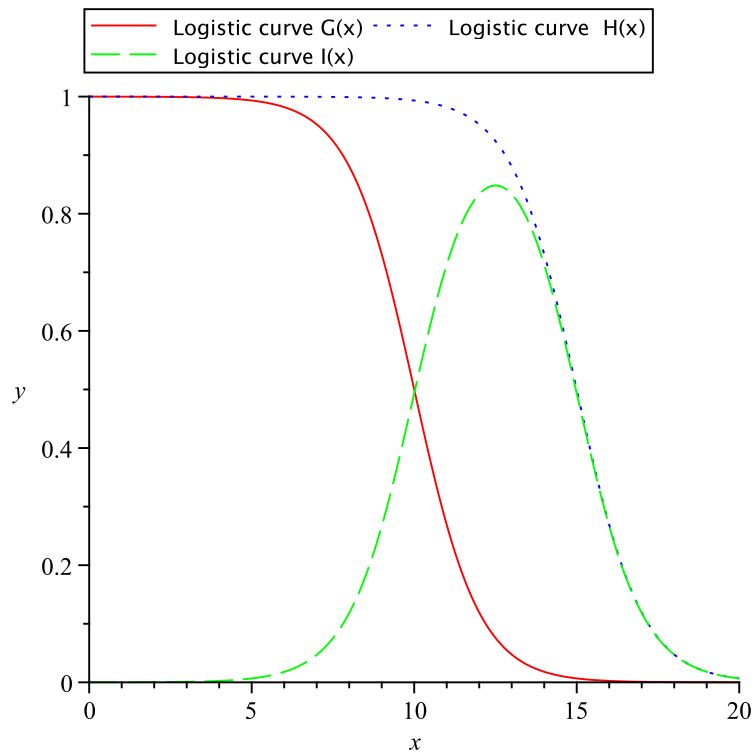
is very similar to that in Fig. 3.8 of the next section.

3.2.3   *Futher manipulation of the logistic equation*

Considering now the following equations:

$$
\begin{aligned}
a(x) &= \frac{1}{1+\exp(-(15-x))} - \frac{1}{1+\exp(-(10-x))} \\
b(x) &= \frac{1}{1+\exp(\frac{-(15-x)}{\sqrt{x}})} - \frac{1}{1+\exp(\frac{-(10-x)}{\sqrt{x}})} \\
c(x) &= \frac{1}{1+\exp(\frac{-(15-x)}{\sqrt{vx}})} - \frac{1}{1+\exp(\frac{-(10-x)}{\sqrt{vx}})}
\end{aligned}
\tag{3.8}
$$

Figure 3.6: A logistic curve to model insects moving into their last life stage.
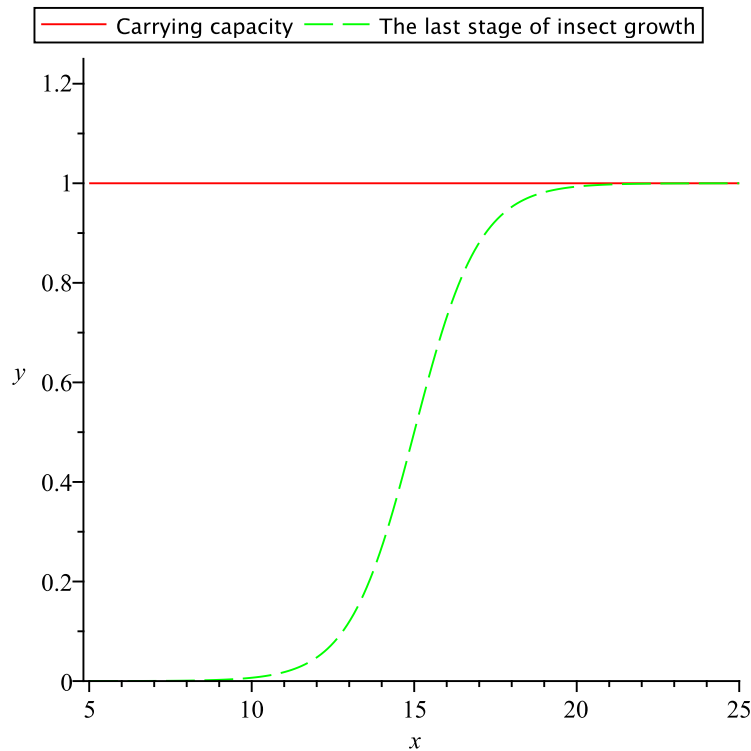
Here $a(x)$ is the logistic equation we have seen thus far. In the formulas for $b(x)$ and $c(x)$, some extra manipulations are made in order to get a form of the logistic equation that appears in Eq. (1.8) of Chapter 1. In $b(x)$ we introduce a division in the exponential by a factor of $\sqrt{x}$. Furthermore, in $c(x)$ we introduce a division in the exponential of $\sqrt{vx}$. Now we have in $c(x)$ the fully constructed logistic equation for the intermediate stages of the logistic model of Eq. (1.8). A plot of the three variants of the logistic equations reveals that as the denominator in the exponential increases, the peak of the intermediate values decreases, and the spread over which insects can occupy a certain life stage also increases. Treatment of the effect of changes in the denominator for the beginning and final life stages of the model are considered in the next section.

It is clear that $b(x)$ is just a special case of $c(x)$ with $v = 1$. Thus, for comparison purposes we need only compare $a(x)$ with $c(x)$. First, we should note that $a(x) > 0, \forall x$,

while $c(x) > 0, x > 0$ since $c(x)$ is undefined when $x \le 0$. Another crucial quality of $c(x)$ is $c(x) \to 0$ as $x \to 0^+$, whereas $a(x) \to 0$ as $x \to -\infty$. This means that $c(x)$ will reach a value in finite time, and $a(x)$ would require infinite time to reach a minimum of zero. This is imporatant biologically because we cannot use infinite time in that regard. This point also lends more credibility to the model with $c(x)$, since it is more realistic than $a(x)$ in a biological sense.

Figure 3.7: A plot of $a(x)$, $b(x)$ and $c(x)$ of equations (3.8).
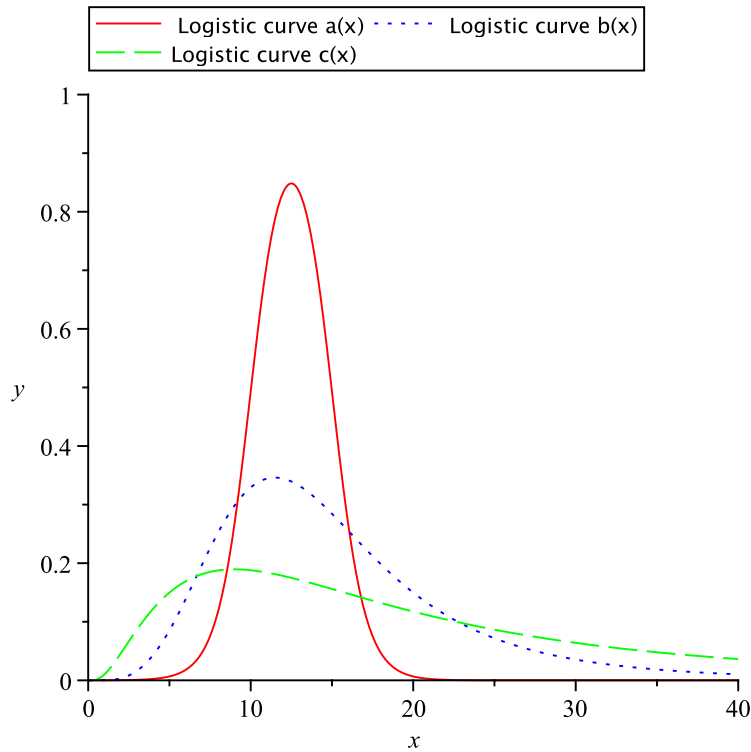
3.3 Traits of the logistic phenology model

A further examination of the traits of the logistic phenology model in Eq. (1.8) of Ch. 1 may be of interest to certain audiences. For example, one may be interested in how the parameters affect the shape or the location of the distribution on a graph. Also, one may be interested in what constraints the model has.

Some of the constraints of the parameters are illustrated here. The values of the a_i's ought to be consecutive. Otherwise, if we had a case where $a_4 < a_3$, then completion of the third instar would occur after completion of the fourth instar. This does not make biological sense, and therefore each successive a_i should be greater than a_{i-1}. More precisely, we ought to have the constraint $0 < a_1 < a_2 < a_3 < a_4 < a_5$. Note that we have the constraint

that $0 < a_1$.

The other parameter v has to be greater than zero. Within Eq. (1.8) we see that v is housed in a square root, and we must have the constraint that $v > 0$ to obtain biologically meaningful results. Once all of these traits are satisfied, we get a population distribution that appears in Fig. 3.8.

Figure 3.8: The logistic phenology model, exhibiting the different instar proportions. Note that $p_1(t)$ contains the proportion of grasshoppers in instar one and below (Dennis and Kemp (1988, [10])).
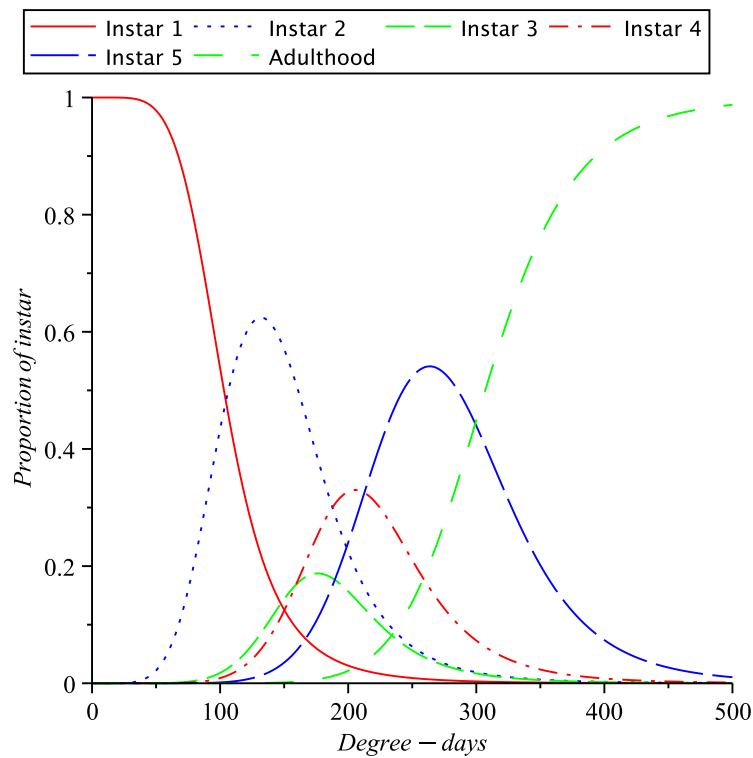
The way that this logistic probability function is defined, we get the condition that

$$\sum_{i=1}^{6} p_i(t) = 1, \ \forall t. \tag{3.9}$$

We get a result of unity when we sum all of the proportions because the sum of the proportions is a telescoping sum.

When analyzing the parameter v, it was found that this parameter controls the variance of the proportions of the grasshoppers in different instars. When analyzing the effect of v on the distributions, three different values of v were taken. In Figs. 3.9, 3.10, and 3.11, we have $v = 0.4$ corresponding to the green graph, which is the dashed-dotted graph. The red graph, which is the dotted graph, pertains to the situation where $v = 4.0$; and finally, the blue-solid graph pertains to the case where $v = 40$. In Fig. 3.9 we have the first portion of the logistic probability distribution plotted, or $p_1(t)$. When the value of v is low, as in the green dashed-dotted line, we get a function that rapidly drops off from a proportion of one to a proportion that approaches zero. For the highest value of v the rate that the function drops from a proportion of one to a proportion of zero has a much greater spread than that of the function with lower values of v. Notice that all the graphs in Fig. 3.9 cross at the same point, at $t = a_1$, which is the point at which the population of grasshoppers in instar one is fifty percent [9] .

In the intermediate stages of the phenology, we can see that we get a greater variance over which the model extends as v increases. Also note that the function has a higher peak when the value of v is decreased. When considering $p_6(t)$, we get the situation that occurs in Figure 3.10. This situation is analogous to that of $p_1(t)$ except the function with a lower value for v will increase from a proportion of zero to a proportion of one very quickly. Also note here that all three curves intersect at the same point, which is a_5, the point where the grasshopper population is at fifty percent adulthood.

51

Figure 3.9: Plots of $p_1(t)$ when v is varied.
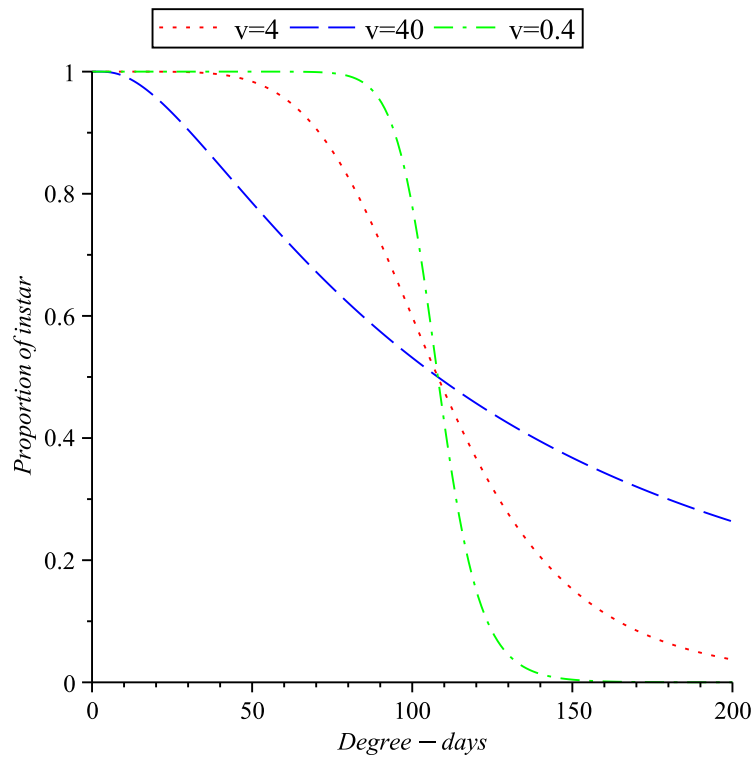
Figure 3.10: Plots of the intermediate stage $p_2(t)$, as v changes.

53
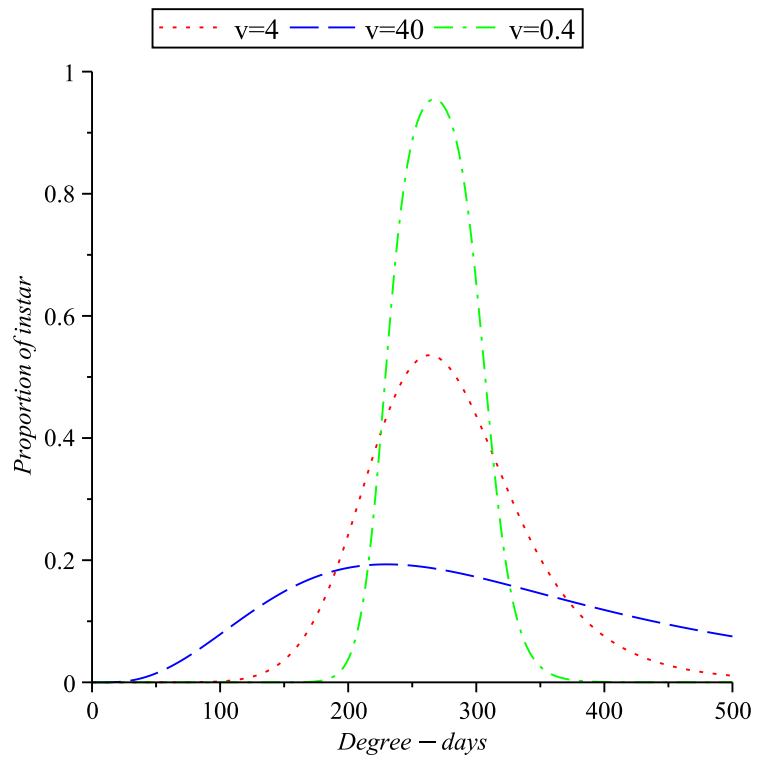
Figure 3.11: Plots of $p_5(t)$ as v varies.
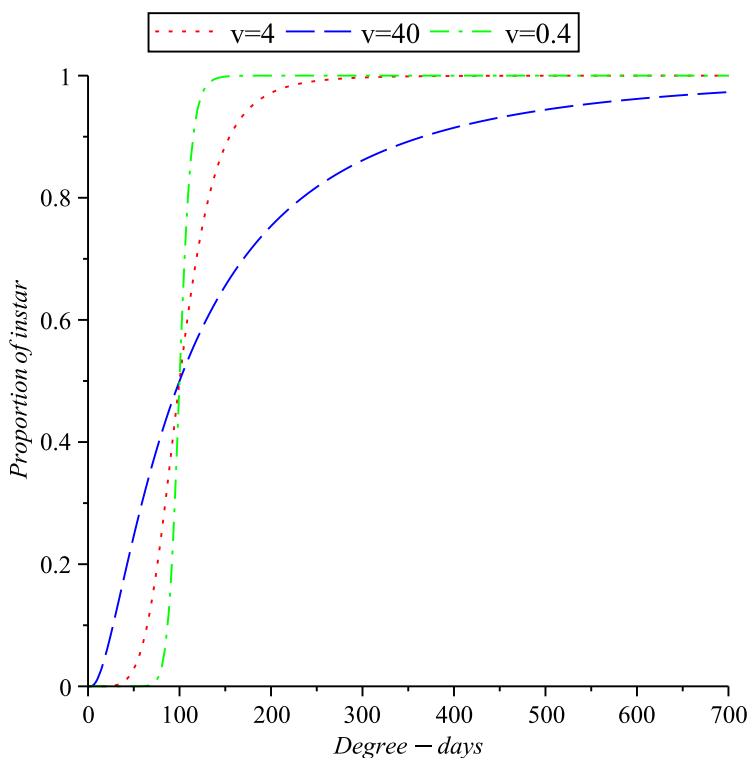
When analyzing how the a_is affect the phenology model it is easy to see that when the a_is have higher values, the logistic probability curves will be shifted to the right. As an example, Fig. 3.12 illustrates how increasing the a_is will shift the curves further and further to the right. In the graph of the dotted red line, $a_2 = 200$ and $a_1 = 100$; $a_2 = 300$ and $a_1 = 200$ in the solid blue curve; and $a_2 = 400$ and $a_1 = 300$ for the green dashed dotted curve. All other things being equal, when we increase the value of the a_is we get curves that are further to the right on a graph of proportion versus degree-days. Also notice that as the curves are shifted further to the right, the peaks of the curves decline.

Another thing to note is the effect of the spread of the different a_is. By inspection, Fig. 3.13, all of the curves have an $a_2 = 300$, whereas in the red dotted, blue solid, and the green dashed-dotted curves the a_1s are 100, 200, and 275, respectively. In these cases, the red dotted curve has the highest peak, but this peak occurs at the lowest value in terms

Figure 3.12: Holding v constant and increasing the a_1 and a_2 values for the intermediate probability $p_2(t)$.
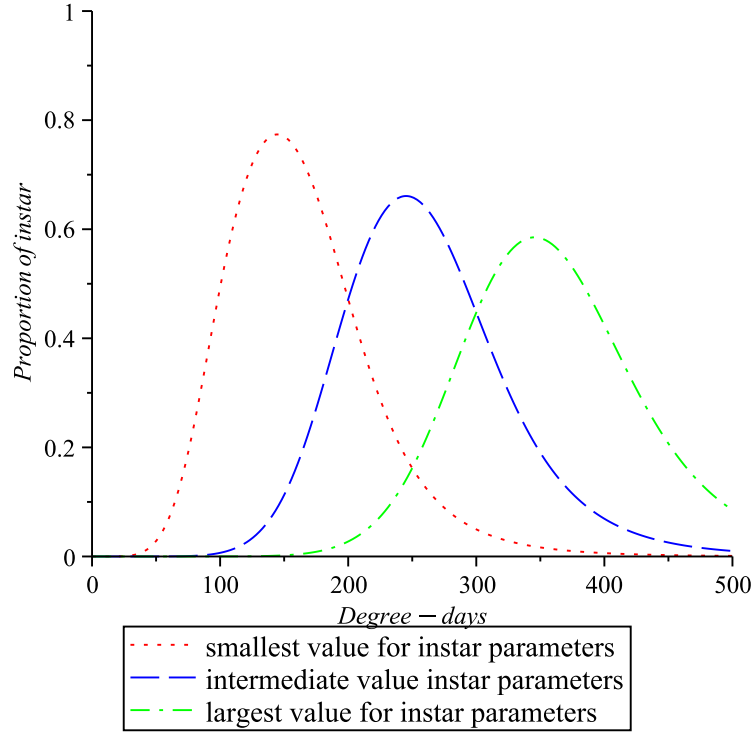
of degree-days. The trend in Fig. 3.13 is that as the distance between a_2 and a_1 is decreased, with a_2 being held constant, the curves have a smaller peak for the proportion of the grasshopper population, and those peaks occur at a higher degree-day value. Also, when observing these graphs, it appears that the peak of these curves occurs approximately around the average of a_2 and a_1.

It is worth mentioning whether or not it is always the case that $p_i(t) \geq 0, \forall t$. It is clearly the case for $p_1(t) = [1 + \exp\left(\frac{-(a_1-t)}{\sqrt{vt}}\right)]^{-1}$. We know that the numerator is always 1, and the denominator will always be 1 or greater since the exponential will always be positive, and will only vanish as $t \rightarrow +\infty$. Therefore, the denominator $1 + \exp\left(\frac{-(a_1-t)}{\sqrt{vt}}\right) \geq 1$, $\forall t$, giving the required condition $p_1(t) \geq 0$, $\forall t$.

For the intermediate stages, we know that $[1 + \exp\left(\frac{-(a_i-t)}{\sqrt{vt}}\right)]^{-1} \geq 0$ $\forall i, t$ and we also

Figure 3.13: A plot illustrating what happens when v and a_1 are held constant and a_2 is allowed to vary.
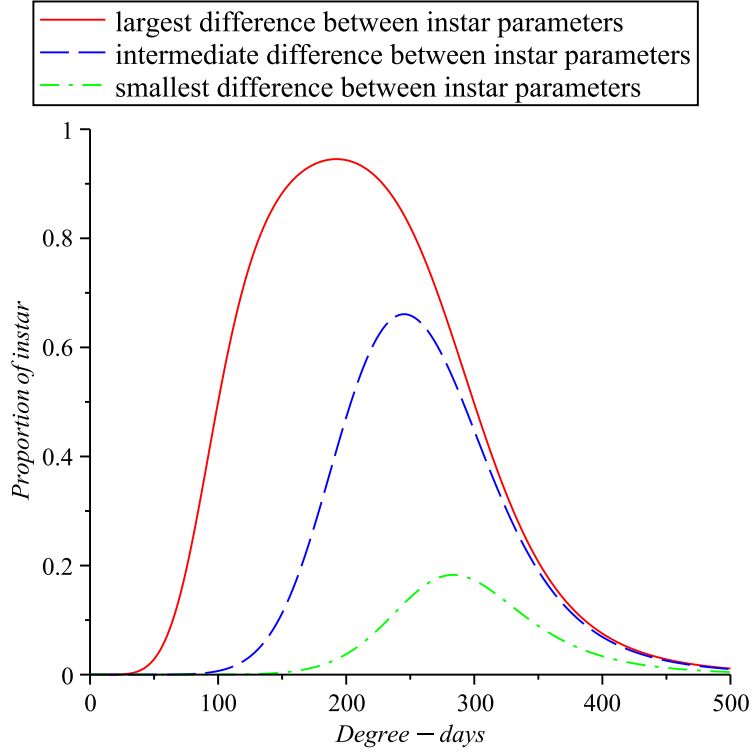
know that $a_i > a_{i-1}$. Thus, all we need to verify is whether the first term is greater than the term being subtracted. Using inequalities, we get:

$$
\begin{aligned}
a_i &> a_{i-1} && (3.10) \\
-(a_i - t) &< -(a_{i-1} - t) \\
\exp\left(\frac{-(a_i - t)}{\sqrt{vt}}\right) &< \exp\left(\frac{(a_{i-1} - t)}{\sqrt{vt}}\right) \\
\frac{1}{1 + \exp\left(\frac{-(a_i - t)}{\sqrt{vt}}\right)} &> \frac{1}{1 + \exp\left(\frac{(a_{i-1} - t)}{\sqrt{vt}}\right)}
\end{aligned}
$$

In the last line of the inequalities of (3.10) we get the desired result, which implies that $p_i(t) \geq 0, \forall t$ in the intermediate cases of the logistic model.

For the final stage of the model we know that the term being subtracted, $\left[1 + \exp\left(\frac{-(a_5 - t)}{\sqrt{vt}}\right)\right]^{-1}$

56

is always greater than or equal to zero. Also, it is apparent that $\exp\left(\frac{-(a_5-t)}{\sqrt{vt}}\right) > 0$, which implies that $[1 + \exp\left(\frac{-(a_5-t)}{\sqrt{vt}}\right)]^{-1} < 1$. Therefore, subtracting this term from 1 will give us the desired result, $p_i(t) \geq 0, \forall t$. Thus the inequality $p_i(t) \geq 0, \forall t$ holds for all stages of the logistic model.

Chapter 4

Fitting the model

4.1 Chapter overview

In this chapter, a general description of nonlinear regression is given, as is a description of the optimization algorithm that my logistic phenology model uses. This chapter analyzes and highlights some of the problems with choosing initial values for parameter estimation within my model. Also, possible solutions to the problem of choosing initial values and solving for the model's parameters are explained.

4.2 Introduction to nonlinear regression

Regression is a mechanism for fitting data to any selected equation. As is the case with a simple linear regression, the goal of nonlinear regression is to find values for parameters that minimize the sum of the squares of the distances of the data points to the curve (Motulsky and Ransas (1987, [49])). If the value for each observation is y_i, and the predicted value for the function is $\hat{y}_i$, the goal is to minimize the sum of squared errors (SSE), with i observations:

$$SSE = \sum_{i=1}^{n} (y_i - \hat{y}_i)^2. \tag{4.1}$$

This method of optimization is known as the least squares method, because the sum of squares of the distances between the observations and predictions is being minimized.

4.2.1 Initial regression attempts

Consider the first part of Eq. (1.8) of Chapter 1:

$$p_1(t) = (1 + \exp(\frac{-(a_1 - t)}{\sqrt{vt}}))^{-1} \qquad (4.2)$$

Regression can be used to determine the values for v and a_1. First, it would be prudent to perform some transformations in order to make the regression more manageable. The transforms are as follows:

$$
\begin{aligned}
q_1(t) &= \frac{1}{p_1(t)} = 1 + \exp\left(\frac{-(a_1 - t)}{\sqrt{vt}}\right) \\
r_1(t) &= q_1(t) - 1 = \exp\left(\frac{-(a_1 - t)}{\sqrt{vt}}\right) \\
s_1(t) &= \ln(r_1(t)) = \frac{t - a_1}{\sqrt{vt}}
\end{aligned}
\qquad (4.3)
$$

Now if we let $u = \sqrt{t}$ and $\beta = \frac{1}{\sqrt{vt}}$ we get the following formula:

$$\hat{\alpha}_1(u) = \beta u - \frac{\beta a_1}{u} \qquad (4.4)$$

Where $\hat{\alpha}_i$ = predicted value (function value) and α_i = the observed value with $u = u_1, u_2, ..., u_n$ and $\alpha = \alpha_1, \alpha_2, ..., \alpha_n$. In this case our SSE_1 becomes:

$$SSE_1 = \sum_{i=1}^{n} (\alpha_i - \hat{\alpha}_i)^2 \qquad (4.5)$$

By expanding the SSE_1 term we get:

$$SSE_1 = \sum_{i=1}^{n} (\alpha_i - \hat{\alpha_i})^2 = \left(\sum_{i=1}^{n} \alpha_i^2 - 2\beta \sum_{i=1}^{n} \alpha_i u_i + \right.$$
$$\left. 2a_1\beta \sum_{i=1}^{n} \alpha_i/u_i + \beta^2 \sum_{i=1}^{n} u_i^2 + a_1^2\beta^2 \sum_{i=1}^{n} 1/u_i^2 - 2\beta^2 a_1 n \right) \qquad (4.6)$$

Now taking partial derivatives of the SSE with respect to a_1 and β, and setting the partial derivatives to zero, we obtain the so-called normal equations:

$$\frac{\partial SSE_1}{\partial a_1} = -n\beta^2 + a_1\beta \sum_{i=1}^{n} \frac{1}{u_i^2} + \sum_{i=1}^{n} \frac{\alpha_i}{u_i} = 0 \qquad (4.7)$$

$$\frac{\partial SSE_1}{\partial \beta} = -\sum_{i=1}^{n} \alpha_i u_i + a_1 \sum_{i=1}^{n} \frac{\alpha_i}{u_i} + \beta \sum_{i=1}^{n} u_i^2 - 2na_1\beta + \beta a_1^2 \sum_{i=1}^{n} \frac{1}{u_i^2} = 0$$

When the above pair of equations with two unknowns are solved, we obtain the following for solutions for β and a_1:

$$a_1 = \frac{n\beta - \sum_{i=1}^{n} \frac{\alpha_i}{u_i}}{\beta \sum_{i=1}^{n} \frac{1}{u_i^2}}$$

$$\beta = \frac{\sum_{i=1}^{n} \alpha_i u_i \sum_{i=1}^{n} \frac{1}{u_i^2} - n \sum_{i=1}^{n} \frac{\alpha_i}{u_i}}{\sum_{i=1}^{n} \frac{1}{u_i^2} \sum_{i=1}^{n} u_i^2 + n^2} \qquad (4.8)$$

Let us continue to use regression to solve for the parameters in the full SSE. We know a_1 and v from our first regression. Now a second SSE (SSE_2) can be set up.

$$SSE_2 = \sum_{i=1}^{j} \left(p_{2i}(t_i) - (1 + \exp(\frac{-(a_2 - t_i)}{\sqrt{vt_i}}))^{-1} \right.$$
$$\left. + (1 + \exp(\frac{-(a_1 - t_i)}{\sqrt{vt_i}}))^{-1} \right)^2 \qquad (4.9)$$

Here, $p_{2i}(t_i)$ is the observed values of the proportion of the population in the second instar

60

at time t_i.

At first glance, SSE_2 seems like it may be a good candidate for a regression in order to solve for a_2. Since we know the values of a_1 and v from the first regression, SSE_2 is just a function of a_2. If we let $x = \left(1 + \exp(\frac{-(a_2 - t_i)}{\sqrt{bt_i}})\right)^{-1}$ and $y = \left(1 + \exp(\frac{-(a_1 - t_i)}{\sqrt{bt_i}})\right)^{-1}$, and take the partial derivative of SSE_2 with respect to a_2, we get

$$\frac{\partial SSE_2}{\partial a_2} = \sum_{i=1}^{j} 2(p_{2i}(t_i) - x + y)\frac{x - 1}{y^2 \sqrt{bt_i}} = 0. \tag{4.10}$$

This is obviously a cumbersome equation to solve, so looking at a numerical method for solving a_2 and successive a_i values seems like a logical option.

4.3 Numerical methods

Most fitting of nonlinear equations to data cannot be solved in one step, unlike the fitting of linear or polynomial equations to data. Fitting nonlinear equations to data must typically be done iteratively. To begin the iterative process, the user of a nonlinear fitting algorithm must supply initial values or guesses for the parameters in the particular equation that is being fitted. The nonlinear regression procedure then adjusts these initial values to improve the fit of the function to the data. The parameters continue to be adjusted to keep improving the fit of the equation to the data. Iterations will continue in the algorithm until negligible improvement of the fit occurs. A tolerance or threshold for improvement is established at the outset of the curve fitting procedure. Once the amount of improvement in the fit of the data falls below the tolerance, the iterations of the procedure are halted, and values for the parameters at last iteration are selected.

61

4.3.1   A downhill simplex method

A downhill simplex method can perform multidimensional minimization. The downhill simplex method does not require the knowledge of the derivative of the function and therefore the method finds frequent use. A simplex is a geometrical figure consisting, in N dimensions, of $N+1$ vertices and all their interconnected line segments and polygonal faces. For example, in two dimensions, a simplex is a triangle and its interior, and in three dimensions, it is a tetrahedron and its interior. In multidimensional minimization it is necessary to give a starting guess, i.e., $N+1$ points that define an initial simplex.

Figure 4.1: An example of a reflection, where the old simplex is comprised of the points x_h, x_s, and x_l. The new simplex is composed of the points x_r, x_s, and x_l.
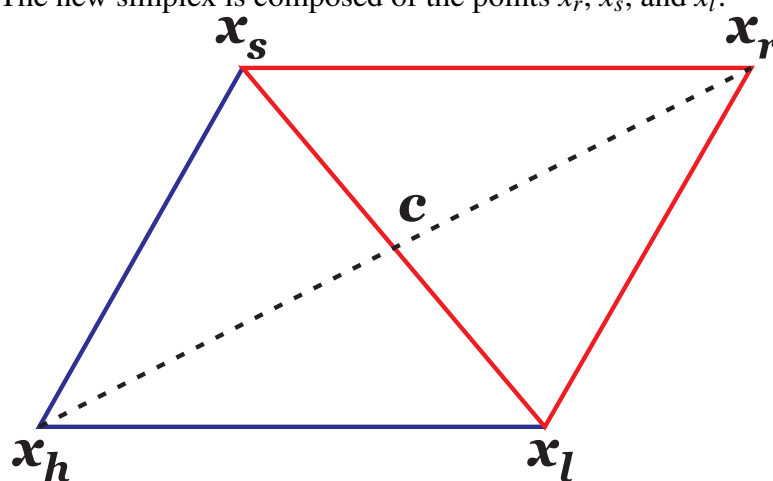
The simplex method takes a series of steps from an initial starting point, through the opposite face of the simplex, to a location where the function has a lower value; these steps are called reflections. The method also can expand itself in one or more directions to take larger steps. When minimization reaches a minimum or valley, the method contracts itself in the transverse direction and tries to go down the valley.

In 1965, Nelder and Mead [53] modified the original method of Spendley *et al.* (1962, [72]) by including two additional transformations. These two new transformations were

Figure 4.2: An example of an expansion of the simplex. The old simplex is as in Fig. 4.1 and the new simplex is x_h, x_s, and x_c.
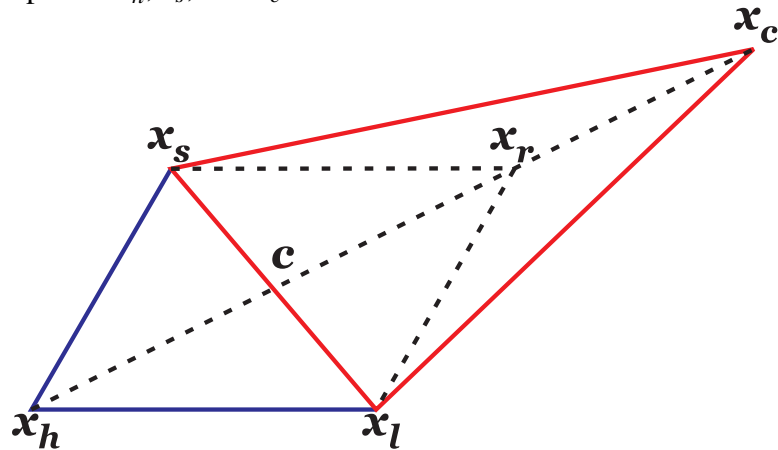
Figure 4.3: An outside contraction of the simplex. The old simplex is as in Fig. 4.1 and the new simplex is x_h, x_s, and x_c.
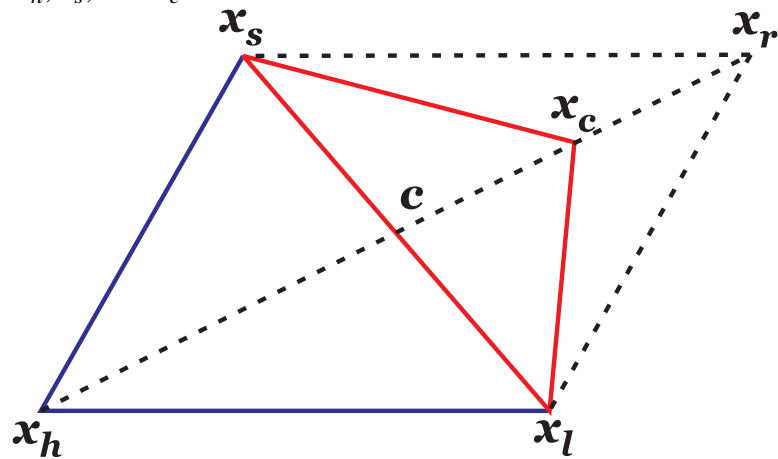
expansion and contraction, that allow the working simplex to change not only its size, but also its shape. By doing so the simplex could adapt itself to the local landscape, elongating down long inclined planes, changing direction on encountering a valley at an angle, and contracting in the neighbourhood of a minimum.

To better illustrate the movements of the simplex, consider a simplex in two dimensional space. In this case, the algorithm first orders the vertices based on the value they produce for the function being minimized. For our example the indices h, s and l refer to

Figure 4.4: An inside contraction of the simplex. The new simplex and old simplex are the same as those in the last figure.
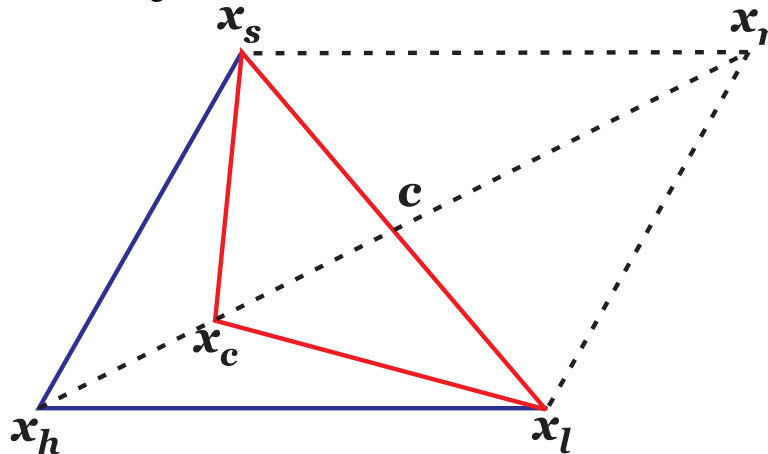
the worst vertex, second worst vertex, and best vertex respectively. The term worst here means that the vertex produces the largest value for the function being minimized, for all the vertices. The vertices associated with these indices are x_h, x_s, and x_l. These vertices in turn produce function values f_h, f_s, and f_l, which correspond to the highest function value, the second function value, and the lowest function value, respectively.

The algorithm now calculates the centroid, c, of the best side. The best side is the one opposite the worst vertex x_h. After the centroid is calculated, the simplex goes through a series of transformations. First a reflection point x_r is calculated and its associated function value f_r. The vertex x_r is accepted if $f_l \leq f_r < f_s$, and the iteration is terminated. The reflection can be seen in Fig. 4.1.

If $f_r < f_l$ an expansion vertex, x_e, is computed along with the function value, f_e, associated with that vertex. If $f_e < f_l$ then the vertex x_e is accepted and the iteration is halted. If $f_e \geq f_r$ then x_r is accepted and the iteration is terminated. The expansion transformation is illustrated in Fig. 4.2.

When the reflections do not work, the simplex will either perform contractions or it will shrink. If $f_r \geq f_s$ then a contraction point, x_c, is calculated. The contraction can be either

Figure 4.5: Shrinking of the simplex. The old simplex is the larger of the two triangles.
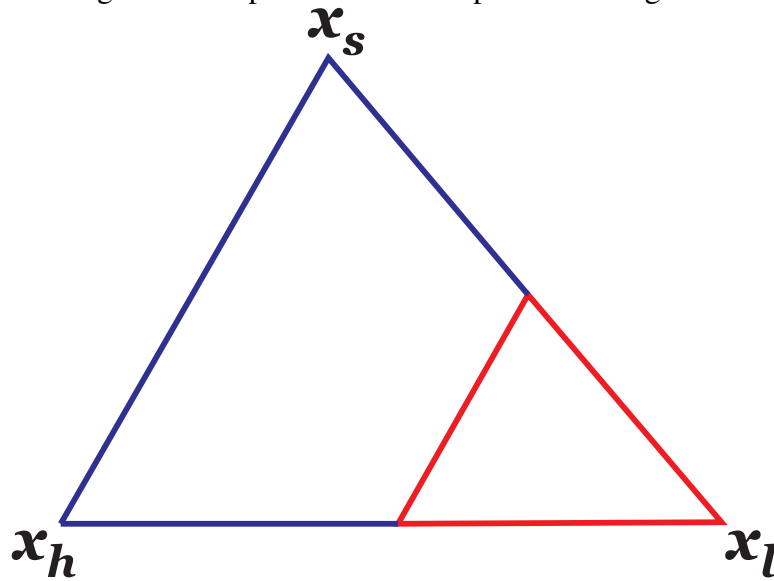
an inside contraction or an outside contraction. If $f_s \leq f_r < f_h$, an outside contraction is computed; and if $f_c \leq f_r$ is accepted then the iteration is terminated. An inside contraction is computed if $f_r \geq f_h$, then if $f_c < f_h$ the inside contraction is accepted and the iteration is terminated. The outside contraction is in Fig. 4.3 and the inside contraction is in Fig 4.4. If either of the contraction points is not accepted then a shrinking of the simplex occurs. The shrink transformation is seen in Fig. 4.5.

Like all minimization algorithms, the convergence criteria can be complicated. Furthermore, since there is more than one variable, it is possible to define different tolerances for each variable, but that was not the method employed in our simplex algorithm. Our method of checking for convergence is to determine when the maximum distance between vertices is lower than some predetermined value (Nelder and Mead (1965, [52]), Olsson and Nelson (1975, [57]), Price *et al.* (2002. [59]), Singer and Singer (2004, [70]), [47]).

4.3.2   *Problems associated with nonlinear regression*

There can be many problems associated with a simplex method when choosing the initial values of the starting simplex, just as there can be some problems associated with choosing initial values for parameters in other numerical recipes for nonlinear optimization. Poor selection of initial values may have some of the following consequences:

1. In a well-behaved system, the amount of computer time required to reach a solution will be increased.

2. Poor choice of initial values may lead the nonlinear regression program to go off in the wrong direction and never converge to a solution.

3. It is also possible that selection of certain initial values can cause the nonlinear program to get trapped in a local minimum which provides incorrect values for parameters.

4.4   Constructing the simplex

When constructing the simplex, values must be chosen for the different vertices of the simplex. Our optimization problem contains six parameters that must be solved for; therefore, we need seven unique vertices for our simplex in order for the algorithm to work correctly.

When choosing initial values for the simplex one must be careful to follow the constraints that each successive a_i is larger than the prior one. We must also have the constraint that all of our parameters are greater than zero.

Implementing initial values of the parameters that do not abide by the constraints $0 < a_1 < a_2 < a_3 < a_4 < a_5$ and $v > 0$ can lead to a variety of situations.

When investigating ways to come up with initial values for the vertices of the starting

simplex, a few methods were examined. In one method we tried to do successive regressions on the $p_i(t)$s. In a sense, we tried to bootstrap our way up through the expressions for the different proportions for the instars and along the way pick off values for v and the subsequent a_is. Starting off with $p_1(t)$, equations for a_1 and v presented themselves. Utilizing the observed instar counts and degree-days accumulated on a certain date for a certain region, we were able to solve for the parameters a_1 and v.

Although the methods for solving a_1 and v are sound, some other problems presented themselves when solving for other parameters. One of the less-than-ideal results that this type of bootstrapping led to was a violation of the constraint $a_{i-1} < a_i$, which is not biologically feasible. Trying to fix the violation of the constraint involved decisions on what data was useful and what data should be discarded. These decisions made the method impractical and convoluted, even for an experienced user; therefore, a more pragmatic approach to the initial value problem for the simplex was needed.

When looking for ways to find a range of the degree-days over which our model is forecasting grasshopper development, one could use the method of moments like approach. For example, we know that parameters a_1 and a_5 correspond to the times when half the grasshopper population is occupied by first instar grasshoppers and adult grasshoppers, respectively. Thus one could find the average of the observed proportions of grasshoppers in these stages, which would be precisely the parameters a_1 and a_5. This method also has some shortcomings with regards to its applicability to timing pest control solutions. One of the disadvantages of this method is that we cannot estimate the parameters for intermediate stages (a_2, a_3, and a_4), nor can we estimate the parameter v. For practical use, there is to be no value added to this model in forecasting a_5 in this manner, since it will occur after the pests are well into adulthood, and the vast majority of damage to crops is done. However, this method can be useful when analyzing historical data in that it would help put a range on starting dates and ending dates during which the majority of pest activity is

taking place, both in Julian and degree-days. Also, the method of moments coupled with historical data could give better indications as to how future grasshopper forecasts might unfold with respect to results typified by certain climatic conditions. Still a simpler method of approximating parameters was needed.

A heuristic method that was tried was an evaluation of a range of degree-days for which some of the instars' populations were peaking in terms of the observations for that day. For example, if we know all of the proportions for our observations, and all of the degree-day accumulations of all the days on which the observations were taken, we could hypothesize about when instar peaks are occurring, or when phenological stages are completing. The advantage of this method is that it allows us to keep the constraints of our parameters intact, since we know the biological meanings of our parameters. We know that a_i is the amount of time required for a grasshopper to complete the ith phenological stage for intermediate instars where $1 < i < 5$. Also, we know that a_1 and a_5 indicate where fifty percent of the grasshopper population is in that instar. Knowing when the molting from one phenological stage to another, or when the instars may be peaking, would then give us a range over which to choose the subsequent a_is for the initial values of the simplex. Even knowing how much heat is required for a grasshopper to graduate from one instar to the next would also allow us to hypothesize a range for the a_is. Based on how fast heat is accumulating for a particular year in which the data is gathered, we could estimate how fast a grasshopper would move through a life stage, which would in turn give us an idea of how the variability of each life stage may look, modelled by the parameter v.

4.5 Analyzing related miniature models

When performing any type of nonlinear regression there is always a chance that the algorithm can converge to a wrong (wrong in terms of the parameters not abiding by their

constraints) local minimum. Knowing that this is a distinct possibility, it may be worth investigating an SSE in order to answer such questions as: Is there one global minimum, and if so, does it abide by the constraints? How many local minima could there possibly be? How should we construct our simplex so we get into a local minimum that gives a feasible or workable solution?

Since we cannot visualize beyond 3-dimensional space, the best way to analyze our 6-dimensional SSE is to look at smaller versions of the optimization problem. This would entail reducing the number of parameters in our model to deal only with a_1 and v, or a_1, a_2 and v. The latter case would be ideal since salient features such as the constraints for successive instars would be retained.

4.5.1 A miniature optimization problem

Before starting the analysis of the full SSE, it is prudent to start first with a very simplistic view of a smaller optimization problem. The first case one could conceivably look at is the case where there are only two parameters, a_1 and v. Biologically, most insects, with a few exceptions, develop from an egg and then have stages where molting occurs [86, 78]. Even though this is a purely biological concern, it can be put aside in the interest of looking at the mathematics, mechanics and features of putting together a model that is a simpler version of our 6-dimensional model. This most miniature version of the full model may enlighten us as to how the larger model is behaving.

Fig. 4.6, is an illustration of what the SSE looks like for the mini-model. The particular SSE for this illustration contains three contrived data points. In Fig. 4.6 we get an idea of how the SSE is shaped. The unlabeled axis is the value of the SSE. In this simplistic model we can see that the SSE is smooth and only appears to have one local minimum.

The particular contrived SSE that gives Fig. 4.6 is

$$
\begin{aligned}
SSE(a_1, v) \;=\;& \left(\left(1+\exp\left(\tfrac{-(a_1-50)}{\sqrt{50v}}\right)\right)^{-1} - 0.85\right)^2 + \left(\left(1 - 1+\exp\left(\tfrac{-(a_1-50)}{\sqrt{50v}}\right)\right)^{-1} - 0.15\right)^2 \\
&+ \left(\left(1+\exp\left(\tfrac{-(a_1-100)}{\sqrt{100v}}\right)\right)^{-1} - 0.7\right)^2 + \left(1 - \left(1+\exp\left(\tfrac{-(a_1-100)}{\sqrt{100v}}\right)\right)^{-1} - 0.3\right)^2 \\
&+ \left(\left(1+\exp\left(\tfrac{-(a_1-200)}{\sqrt{200v}}\right)\right)^{-1} - 0.2\right)^2 \\
&+ \left(1 - \left(1+\exp\left(\tfrac{-(a_1-200)}{\sqrt{200v}}\right)\right)^{-1} - 0.8\right)^2.
\end{aligned}
\tag{4.11}
$$

The degree-days contrived here are 50, 100 and 200 degree-days respectively. The corresponding p_1s for those respective degree-days are 0.85, 0.7 and 0.2. Also the corresponding p_2s are 0.15, 0.3 and 0.8. Also note that in this model the insect being modelled can only be in one life stage, hence the population is always in the first instar. Not much insight can be gathered from this mini-model; thus, considering a model with more parameters would be the next option. With larger optimization models, as the value of v gets smaller, there are more local minima where a simplex might get trapped.

4.5.2   Another miniature optimization

The next logical step is to look at a model with parameters a_1, a_2 and v. Also, in this model the constraints $a_2 > a_1$ and $v > 0$ can both be imposed. With this model, we can contrive data, create different situations, and study the SSE for local minima. Also, by holding one parameter constant, we can look at other parameters and 3-dimensional plots of parameters that are allowed to vary, and see what happens to the shape of the SSE. Even with the 3-dimensional plot, we can only surmise how the surface of the SSE may look in four dimensions. Since we cannot view 4-dimensional space, there may be occurrences when the simplex gets trapped in local minimum with an improper solution, with respect

Figure 4.6: A look at the SSE from a vantage point outward from the origin and the v-axis. The unlabeled axis is the value for the SSE.
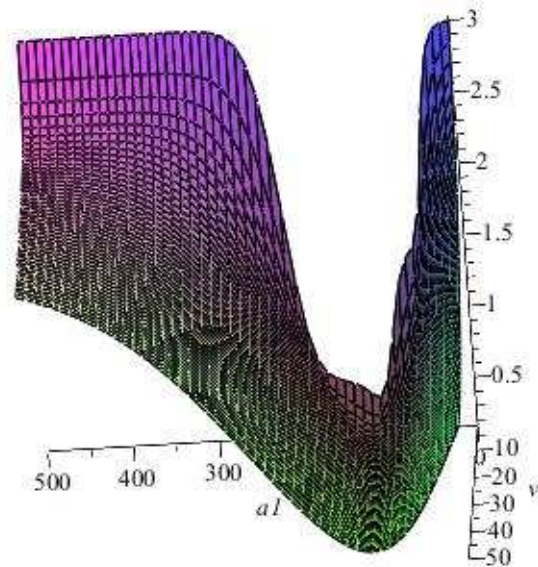
to the parameters and their constraints. However, this analysis may provide information regarding a suitable region to construct the simplex in.

When investigating the SSE below, a_1 and a_2 were allowed to vary while keeping v constant at 20 initially. This yielded illustrations where the surface of the SSE is very smooth. However, when we change the value of v to $v = 1$, situations arise where there are many minima as in Figs. 4.7 and 4.8. In these figures we can see that there are many more peaks and valleys. In this instance, a simplex could easily get trapped in different minima, depending on where the simplex starts, and could subsequently give extraneous solutions

71

for the parameters. The SSE in Eq. 4.12 is a function of a_1 and a_2 with $v = 1$ and is

$$
\begin{aligned}
SSE(a_1, a_2) \quad &= \left(\left(1 + \exp(\tfrac{-(a_1-50)}{\sqrt{50}})\right)^{-1} - 0.85 \right)^2 \\
&+ \left(1 - \left(1 + \exp(\tfrac{-(a_2-50)}{\sqrt{50}})\right)^{-1} - 0.04 \right)^2 \\
&+ \left(\left(1 + \exp(\tfrac{-(a_2-50)}{\sqrt{50}})\right)^{-1} - \left(1 + \exp(\tfrac{-(a_1-50)}{\sqrt{50}})\right)^{-1} - 0.11 \right)^2 \quad (4.12) \\
&+ \left(\left(1 + \exp(\tfrac{-(a_1-100)}{\sqrt{100}})\right)^{-1} - 0.7 \right)^2 \\
&+ \left(\left(1 + \exp(\tfrac{-(a_2-100)}{\sqrt{100}})\right)^{-1} - \left(1 + \exp(\tfrac{-(a_1-100)}{\sqrt{100}})\right)^{-1} - 0.2 \right)^2 \\
&+ \left(1 - \left(1 + \exp(\tfrac{-(a_2-100)}{\sqrt{100}})\right)^{-1} - 0.1 \right)^2 \\
&+ \left(\left(1 + \exp(\tfrac{-(a_1-200)}{\sqrt{200}})\right)^{-1} - 0.1 \right)^2 \\
&+ \left(\left(1 + \exp(\tfrac{-(a_2-200)}{\sqrt{200}})\right)^{-1} - \left(1 + \exp(\tfrac{-(a_1-200)}{\sqrt{200}})\right)^{-1} - 0.5 \right)^2 \\
&+ \left(1 - \left(1 + \exp(\tfrac{-(a_2-200)}{\sqrt{200}})\right)^{-1} - 0.4 \right)^2
\end{aligned}
$$

Inspection of the SSE shows that the three data points have degree-day values of 50, 100, ad 200 respectively. The corresponding p_1s for these degree days are 0.85, 0.7, and 0.1 respectively. The p_2s are 0.11, 0.2 and 0.5 while the p_3s are 0.04, 0.1 and 0.4.

Noting that valleys become more prevalent as the value of v gets very small, one lesson we could take away from looking at the miniature model is to have initial guesses for the parameter v starting away from relatively low values such as $v \leq 1$. Some researcher (Onsanger and Kemp (1986, [54]), and Dennis *et al.* (1986, [9])) have found v with lower bounds of at least 4 for some species of grasshoppers, which lends some plausibility to constructing a simplex away from lower values of v. In the next chapter, there will be a further discussion of parameters that we obtained compared to parameters that other researchers

have obtained.

Another variable that affects the complexity of the SSE is the number of data points sampled. The SSE surface will generally get more complex as more data points are taken into consideration. For example, we can compare and contrast Fig. 4.7 and Fig. 4.8. In Fig. 4.7 we have the SSE with three data points that was already listed for this miniature model. In Fig. 4.8 note that there are a total of six data points. The surface of the SSE in Fig. (4.10) is more complex in the sense that the surface seems crumpled and has more distinct valleys in which a simplex might be caught.

Figure 4.7: The surface of an SSE with only three data points, from our mini-model with parameters a_1, and a_2 varying with v=1.
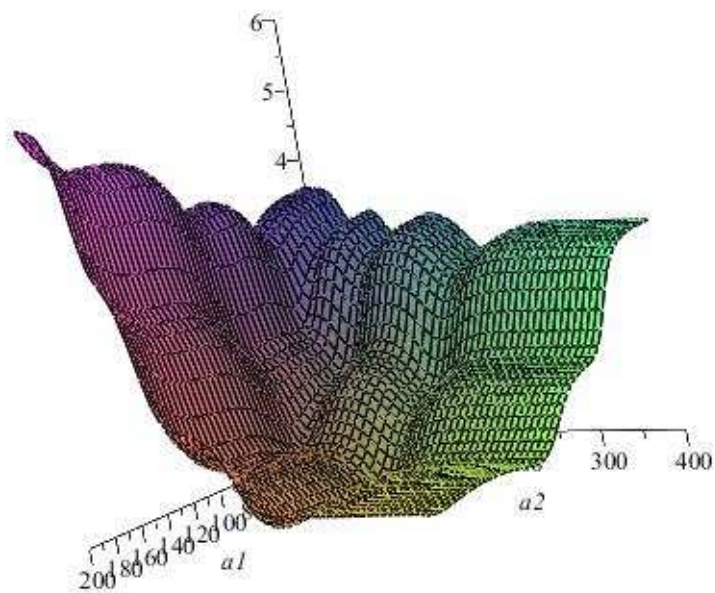
Figure 4.8: The surface of an SSE with six data points, again allowing a_1 and a_2 to vary while keeping $v=1$. The surface seems generally more complex than in Fig. 4.7. The a_1 axis is the left axis in this illustration whereas the a_2 axis is the right axis. The vertical axis is the value of the SSE.
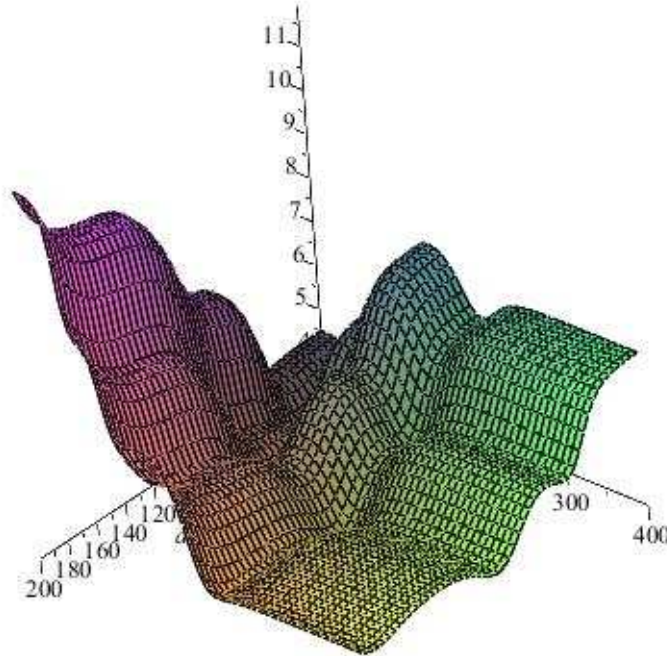
4.6   SSE for the full model

In the full model, there is a total of six parameters. The parameters a_1 through a_5 are measures of phenological growth of the grasshoppers, and v is related to the duration that a grasshopper can occupy a certain phenological stage in terms of degree-days. Again, we cannot visualize what the surface of the SSE would look like in 6-dimensional space; however, the SSE can be viewed while holding four parameters constant and allowing the other two parameters to vary.

When looking at the SSE, there was interest to see how it would react if v was varied. By inspecting the 3-dimensional figures for the SSE, it became clear that as v decreased in value, there was an increase in the number of local minima that were occurring.

74

Figure 4.9: Here $v = 1$ and we can see that there are peaks and valleys occurring.
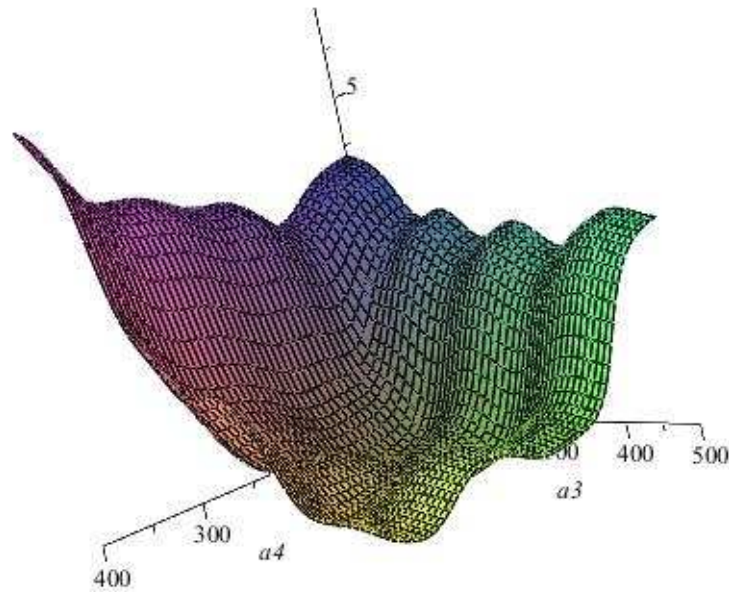
In Figs. 4.9 and 4.10, we are allowing a_3 and a_4 to vary while having $v = 1$ and $v = 0.5$, respectively. These two cases have more than one local minimum as compared to the case where $v = 20$. Also as v decreases from 1 to 0.5, the minima are more pronounced; that is, the valley floors contain steeper walls. This conclusion is apparent in comparing Figs. 4.9 and 4.10. Also note that in this full model, the SSE is comprised of six data points, but the equation for the particular SSE is not listed because it is very large.

The same conclusion can be made from analysing both the miniature model and the full model. When constructing a simplex, the values corresponding to the parameter v ought to be away from lower values. Having v start further away from lower values in turn helps the simplex to avoid the region where the SSE surface has many local minima. In our case we should not begin with simplex values of v close to 1, but further out, such as $v = 5$ or greater in order to maintain an SSE that has a surface with possibly fewer local minima.

Figure 4.10: In this figure $v = 0.5$, and we are looking at the surface of SSE. The unlabeled axis is the value of the SSE. The peaks and valleys seem more pronounced here than in Fig. 4.9.
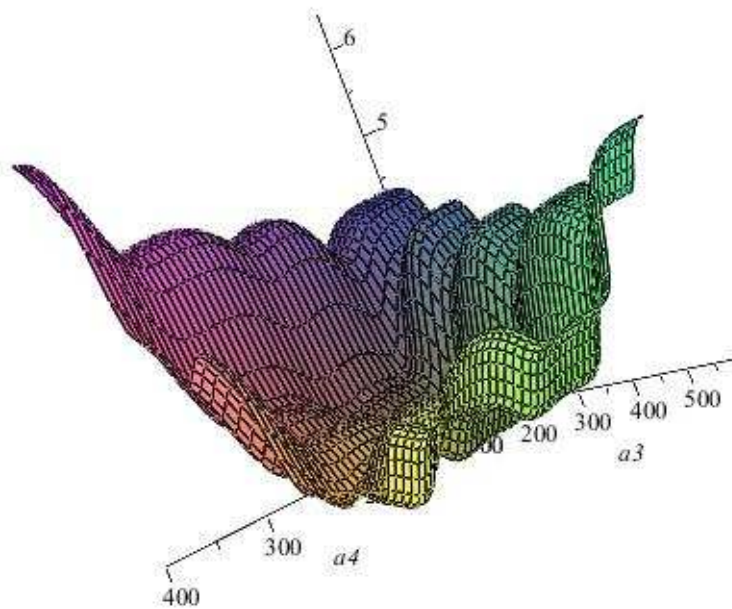
Chapter 5

Results and conclusions

5.1 Chapter overview

The final model uses the improved degree-day accumulators developed in Chapter 2, and analysis of Eqn. (1.8) that was done in Chapter 3. Also, while developing and testing the final model, Chapter 4 was necessary in order to inform readers of the process and some of the problems encountered when using the final model. Chapter 5 explains some of the data that was used when running our logistic phenology model, and some prior work done using this model. Also this chapter gives some suggestions that researchers may want to take into account when using this model in the future.

5.2 Running the logistic phenology model with real data

One species of grasshopper with available data was *Melanoplus sanguinipes*. This species was observed in the vicinity of the town of Onefour, located in southwestern Alberta. The observations were made between June and September 2000, for six particular dates. When running our simplex method for finding the six different parameters, we used a development threshold of 12 °C. The results obtained for each of the different degree-day accumulators are listed below in Table 5.1.

Table 5.1: Parameters estimates for *M. sanguinipes* at Onefour for the year 2000.

Degree-day method	a_1	a_2	a_3	a_4	a_5	v
Linear heating and cooling	105.33	197.95	355.71	473.92	549.94	27.83
Traditional sine	110.12	203.69	358.75	491.67	575.38	27.56
Sine heating and linear cooling	108.65	200.71	357.32	481.53	565.49	28.78
Sine heating and cooling	111.21	203.02	357.43	495.28	578.46	26.93

The values of the a_i parameters are fairly consistent throughout the analysis, with the biggest gap of ≈ 28 degree-days between the a_5 values when comparing the linear heating and cooling accumulator and the sinusoidal heating and cooling accumulator. The difference in the highest and lowest values for the parameter v was 1.85.

5.3   Comparisons to other studies

The species *M. sanguinipes* was also studied by Onsanger and Kemp (1986, [54]) using the same model. The collection of their grasshopper data was done in approximately weekly intervals during the summer months of 1975 and 1976 near Roundup, Montana. In the year 1975, grasshoppers were collected for 22 weeks, and in 1976, grasshoppers were collected for 19 weeks. Thus, Onsanger and Kemp have 22 and 19 observations respectively, compared with our six observations for the year 2000 at Onefour, Alberta. Also, there is a geographical difference in that Roundup, Montana, is located approximately 415 km southwest of Onefour, Alberta.

Table 5.2: Grasshopper counts (*M. sanguinipes*) at Onefour for the year 2000, for six different dates.

Date	Instar 1	Instar 2	Instar 3	Instar 5	Instar 5	Adult	Total
June 22nd	34	59	118	17	1	0	229
July 6th	20	26	39	22	9	1	117
July 18th	8	59	74	27	31	24	223
August 1st	0	9	32	24	17	35	117
August 15th	0	0	3	17	23	89	132
September 9th	0	0	0	0	1	39	40

There were several other differences in methodology of collecting data that can account for differences in the parameters obtained from our model and that of Onsanger and Kemp. One of these was that Onsanger and Kemp recorded air temperature at 5cm above ground, whereas our temperature was obtained 2m above ground. Also, Onsanger and Kemp used

only the traditional sine wave method for calculating degree-day accumulations, with a developmental threshold of 17.8 °C. Our model contains four methods for calculating the degree-day accumulation, with a threshold of 12 °C. Another difference is that they started their accumulation of degree-days on May 6th of each year. Our model can take into account degree-day accumulation for the whole year, but typically degree-day accumulations begin on April 1st of the year. Also, the traditional sine wave method for degree-day accumulation does not take into account the geographic location of the grasshopper observations, nor the daily temporal aspect of heating and cooling that occurs during the day. Differences in biofix dates and temperature thresholds come from difference in preferences, location, and laboratory results that different researchers use (Hewitt (1979, [20]), Kemp (1987, 1989, [32], [34]), Kemp and Dennis (1991, [35]).

The parameters for Onsanger and Kemp's work are in Table 5.2. As shown, the a_i val-

Table 5.3: Parameter estimates for *M. sanguinipes* for the years 1975 and 1976 near Roundup, Montana.

Year	a_1	a_2	a_3	a_4	a_5	v
1975	54.66	111.85	148.45	199.89	287.99	5.19
1976	80.76	124.96	168.86	283.54	391.61	9.99

ues obtained by Onsanger and Kemp are much lower than our a_i values. This is likely due to Onsanger and Kemp using such a high threshold of 17.8°C. By using a lower threshold like 12 °C, Onsanger and Kemp would have gotten higher a_is (since more degree-day accumulation would occur), and consequently it would imply that the grasshoppers were spending more time (in terms of degree-days) in a certain phenological stage. This would, in effect, increase the spread of the logistic curves, and subsequently, Onsanger and Kemp would have obtained a higher v value, with a lower developmental threshold.

One comparison is to take a developmental threshold of 17.8°C and run the model using our degree-day accumulators. To do this, the initial values for our simplex must

be augmented to take into account a higher threshold resulting in lower accumulations occurring when compared to a threshold of 12 °C. Here again we are using the same data for Onefour from the year 2000. We obtain the following:

Table 5.4: Parameter estimates for *M. sanguinipes* at Onefour for the year 2000, using a threshold of 17.8 °C.

Degree-day method	a_1	a_2	a_3	a_4	a_5	v
Linear heating and cooling	1.29	76.79	138.87	159.84	161.32	2.03
Traditional sine	5.28	91.29	137.39	213.97	246.77	1.59
Sine heating and linear cooling	13.26	67.24	132.45	188.92	193.15	1.57
Sine heating and cooling	13.41	99.30	151.73	187.91	225.33	1.70

Comparing this table with Table 5.2, we can see that the v values are lower than those achieved by Onsanger and Kemp. Here we can also see that the parameter a_1 has low values, and it seems implausible to have such small values for the first phenological stage. However, the comparison for this parameter can be problematic, since we are at a different geographic location during a different year. Also, the other parameters in table 5.3 have lower values than Onsager and Kemp's work.

5.3.1 Problems with comparing data

There are many potential differences in the ways the data was collected between our model and the Onsanger and Kemp model, our comparison relates only to the basic differences in the temperature and values of the parameters. Also, the grasshopper counts and temperature data that Onsanger and Kemp used are not available. Moreover, there is no information readily available on what they used for initial values for their simplex in the Nelder-Mead algorithm. Thus, we are not in a position to either refute or confirm their results.

Although authors like Onsanger, Kemp, and Dennis derived this logistic phenological model, they do not mention some of the difficulties involved with using the Nelder-Mead

algorithm that this thesis discusses. For reasons unknown, these authors do not give a rigorous mathematical treatment of the model. For example, their papers on this model do not mention the pitfalls of a simplex falling into a local minimum that may give extraneous parameters. Although the constraints for the parameters might be implied in their papers, they are never directly expressed.

5.4 Improvements and future work

One possible way to improve upon this model is to reduce the number of parameters in the model, thus making the SSE less cumbersome. The duration that a typical pest grasshopper spends in the first instar is very short (Johnson 2008, [29]); thus, we could pool the first and second instar grasshoppers into one category, thereby combining a_1 and a_2 into one category. By doing this, we would reduce the complexity of the SSE and perhaps get a more accurate range over which the first and second instars may be occurring.

Other intermediate stages could be pooled together, depending on the researcher's needs, which may benefit his or her work. For example, a researcher may want to group the first and second instar together, and the third and fourth instar together, thereby reducing the minimization problem from six parameters to four parameters. This may add value to those researchers who are concerned with pest management strategies and schedules, in that they may lump together instars in which the grasshopper is most voracious, thus giving a better time frame in which to apply pesticides.

Pooling of instars ought to be used with caution, however. The parameter v is a measure of dispersion of the instars that remains constant throughout the use of the model. Obviously, when two or more instars are pooled, it increases the amount of the time that the grasshoppers will be spending in the hybrid instar, thereby changing v for the whole model. Thus, one ought to take caution when attempting to pool instars, since such changes will

affect the resulting parameters.

Because information is the prime driver for the majority of models and confidence is created by replication, another way to improve this model would be to gather more data from different locations during different years and run the model against this new data in order to make more comparisons. Also, by gathering more historical data and running the model with said data, we can test what the model is predicting versus what actually happened in the field. By doing so, the model can be refined in order to become more robust and precise.

The task of collecting grasshoppers and properly identifying them is a time-consuming and laborious task, and could be a potential barrier for any kind of model involving the phenological stages of the grasshopper. Moreover, gathering all the weather data for the corresponding collection of grasshopper data is also very time-intensive. The cost and manpower needed to accomplish these things could hinder improvements to the model, in terms of gathering more data. One way to reduce the manpower needed to do this task would be to take roadside survey counts (Johnson (1989, [30])).

Another potential hurdle to this model is that a general user may not be familiar with the constraints necessary when determining the values for the initial simplex. By having experts put into place hard coded data for different scenarios, the problem of selecting the initial values for the simplex could be overcome. However, this comes at the price of gathering more data, more comparisons and more manpower.

Improvements in gathering temperature data could also contribute improvements for this model. For example, if temperatures are taken not only at 2m but at 5cm above the ground, researchers would have a better estimate of what is going on in the micro-climate in which the grasshoppers live.

Other future work that this model could produce is a stochastic phenology model for other insects that have temperature as their primary driver for growth. The code for this

model is very general, and we used data for grasshoppers; however, it can be used to model other organisms that have temperature-driven growth and activities.

Working with this model first hand, I observed that it has limitations in that it can be very time intensive to model even one set of data point for one location. This results from time devoted to choosing initial values for parameters in the simplex, and also requiring the acquistion of data from the field. Acquistion of field data for a large variety of habitats, and for a variety of dates would also be time consuming. The conversion of temperature to degree-days is also time consuming in that the temperature data must be formatted properly to be used in conjunction with our program.

To overcome these hurdles future researchers could use the Lactin and Johnson model since it only relies on temperature, and four parameters for each life stage [37]. The beauty of this model is that once the paramters are determined, whether it be in the laboratory or field, they do not need to be recalculated. With the logistic phenology model, the parameters must be calculated evertime the model is run. Thus, the Lactic and Johnson model has the potential to expedite the modeling process since it would not require calculating initial cvalues for a simplex, nor would it require a conversion to degree-days. One lengthy component of modeling that would remain the same would be the collection of the weather data from available sources.

Appendix A

Widespread use of degree-days

United States:

Alabama:

Hendricks, Harlan J., and M. L. Williams. 1992. Life history of *Melanaspis obscura* (Homoptera: Diaspididae) infesting Pine Oak in Alabama. *Entomological Society of America*. 85(4): 452-457.

Connecticut:

Kingsolver, J. G. 1989. Weather and the population dynamics of insects: integrating physiological and population ecology. *Physiological Zoology*. 6(2): 314-334.

http://www.jstor.org/stable/30156173

Hawaii:

Vargas, R. I., W. A. Walsh, E. B. Jang, J. W. Armstrong, and D. T. Kanehisa. 1996. Survival and development of immature stages of four Hawaiian fruit flies (Diptera: Tephritidae) reared at five constant temperatures. *Entomological Society of America*. 89(1): 64-69.

Illinois:

Gu, W. D. and R. J. Novak. 2006. Statistical estimation of degree days of mosquito development under fluctuating temperatures in the field. *Journal of Vector Ecology*. 31(1): 107-112.

Changnon, D., M. Sandstrom, and J. Astolfi. 2010. Using climatology to predict the first major summer corn earworm (Lepidoptera: Noctuidae) catch in north central Illinois. *Meteorological Applications*. 17(3): 321-328.

Kansas:

Charlet, L. D. 1987. Emergence of the sunflower stem weevil, *Cylindrocopturus adspersus* (Coleoptera: Curculiondae), relative to calendar date and degree-days in the Northern Great-Plains. *Journal of the Kansas Entomological Society*. 60: 426-432.

Kentucky:

University of Kentucky summary of insect degree day models:

http://www.ca.uky.edu/agc/pubs/id/id93/app.pdf

Nebraska: Stilwell, A. R., R. J. Wright, T. E. Hunt. 2010. Degree-day requirements for alfalfa weevil (Coleoptera: Curculionidae) development in eastern Nebraska. *Environmental Entomology*. 39(1): 202-209.

New Hampshire:

Use of growing degree-days for insect management:

http://extension.unh.edu/agric/GDDays/Docs/growch

Ohio:

Insect degree-day websites used in Ohio:

http://www.entomology.umn.edu/cues/Web/049DegreeDays.pdf

http://www.ipm.msu.edu/landscapeipm/gddarticle.htm

http://extension.entm.purdue.edu/publications/B504.pdf

Oregon:

Insect degree-day websites used in Oregon:

http://climate.usurf.usu.edu/includes/pestFactSheets/degree-days08.pdf

http://www.fs.fed.us/pnw/pubs/pnwrn482.pdf

Pennsylvania:

Georgian, T. and B. Wallace. 1983. Seasonal production dynamics in a guild of periphyton-grazing insects in a southern Appalachian stream. *Ecology*. 64: 1236-1248.

Utah:

Using degree days to time treatments for insect pests. Utah State University website: http://climate.usurf.usu.edu/includes/pestFactSheets/degree-days08.pdf

Washington:

Olsen, K. N., W. W. Cone, and L. C. Wright. 1998. Influence of temperature on grape leafhoppers in south central Washington. *Environmental Entomology.* 27: 401-405.

West Virginia:

Rock, G. C., R. E. Stinner, J. E. Bacheler. 1993. Predicting geographical and within-season variation in male flights of 4 fruit pests. *Environmental Entomology.* 22: 716-725.

Wisconsin: Insect degree-day website used in Wisconsin:

http://www.entomology.wisc.edu/cullenlab/insects/degreedays.html

Wyoming:

Brewer, M. J., and K. M. Hoff. 2002. Degree-day accumulation to time initiation of sampling for alfalfa weevil using on-site, near-site, and regional temperature data. *Journal of Agricultural and Urban Entomology.* 19: 141-149.

Canada:

Ontario:

Laing, J. E. and J. M. Heraty. 1984. The use of degree-days to predict emergence of the apple maggot, *Rhagoletis pomonella* (Diptera: Tephritidae), in Ontario. *Canadian Entomologist*. 116: 1123-1129.

Laing, J. E. and J. A. K. Reid. 1976. Developmental threshold and degree-days to adult emergence for overwintering pupae of apple maggot Rhagoletis pomonella (Walsh) collected in Ontario.*Proceedings of the Entomological Society of Ontario*. 107: 19-22.

Quebec:

Boivin, G. and D. L. Benoit. 1987. Predicting onion maggot (Diptera: Anthomyiidae) flights in southwestern Quebec using degree-days and common weeds. *Phytoprotection*. 68: 65-70.

Alberta, Saskatchewan, Manitoba:

Insect Pest Monitoring Network (IPMN)

http://www.westernforum.org/IPMNMain.html

International cases:

Brazil:

Neves, A.D., M. D. Haddad, N. G. Zerio. 2010. Temperature requirements and generation number estimates of croton mealybug reared in Rangpur lime. *Pesquisa Agropecuaria Brasileira*. 45: 791-796.

Appendix B

A comparison of degree-day accumulation methods for various years on the Canadian Prairies.

The following is a list of cities across the Canadian Prairies, and a comparison of three different types of degree-day accumulators and the total degree-day accumulation that occured for each year. The three accumulators are the temporal sine method which was constructed for the logistic phenology model outlined for this thesis. The other accumulators are the traditional sinusoidal accumulator, and the average method for degree-day accumulation. As can be seen, the average method consistently underestimated the amount of degree-day accumulation when compared with the other two degree-day accumulators. The threshold used for these accumulations in 12 °C. The first table is an example of the degree-day accumulations for specific days in Lethbridge, Alberta for 1970. Note that this specific data was collected for each of these days, for the years 1970 through 2006 for all the cities which have yearly summaries, but was excluded from this appendix due to the magnitude of the data. Also note that when information was not available for a year, a dash appears in the tables that follow.

Table B-1: Degree-day accumulations for Lethbridge, Alberta, for specific days in 1970.

Day	Temporal sine method	Traditional sine method	Average method
April 1	0.0	0.0	0.0
April 15	3.3	0.0	0.0
May 1	3.4	0.0	0.0
May 15	28.4	25.2	91.1
June 1	81.1	79.0	42.1
June 15	171.4	171.9	122.5
July 1	279.5	289.9	233.8
July 15	384.0	400.0	338.3
August 1	526.0	547.0	477.2
August 15	634.0	658.6	580.5
September 1	769.0	790.0	631.5
December 31	922.0	947.0	800.4

Table B-2: Degree-day accumulations for Lethbridge, Alberta, from 1970 to 2006.

Year	Temporal sine method	Traditional sine method	Average method
1970	922.0	947.0	800.4
1971	871.7	878.0	703.9
1972	751.0	750.0	590.2
1973	650.2	848.7	680.1
1974	800.0	800.0	610.6
1975	707.2	715.3	564.7
1976	828.8	807.3	615.3
1977	708.2	702.0	503.1
1978	723.0	728.8	558.7
1979	860.0	859.9	961.2
1980	790.8	784.4	584.0
1981	806.4	809.2	619.6
1982	744.0	750.4	577.9
1983	826.7	837.9	656.0
1984	829.2	839.1	689.7
1985	752.0	748.7	554.1
1986	785.1	784.8	607.4
1987	871.1	863.8	622.4
1988	973.0	977.5	767.9
1989	778.7	776.8	599.2
1990	840.5	849.8	674.2
1991	822.8	824.9	647.8
1992	781.0	780.0	575.0
1993	576.7	563.3	370.1
1994	851.1	839.2	615.8
1995	649.7	634.3	428.1
1996	838.1	842.6	661.1
1997	825.0	819.1	624.7
1998	930.9	929.2	721.1
1999	731.7	709.5	458.5
2000	848.7	834.6	610.7
2001	948.9	940.0	711.8
2002	675.0	674.3	525.6
2003	937.9	934.6	733.3
2004	727.7	713.6	468.2
2005	681.7	660.5	417.7
2006	866.0	862.6	675.0

Table B-3: Degree-day accumulations for Medicine Hat, Alberta, from 1970 to 2006.

Year	Temporal sine method	Traditional sine method	Average method
1970	1010.4	1032.9	882.8
1971	981.6	989.9	802.8
1972	907.2	916.8	740.8
1973	950.1	948.3	742.3
1974	911.1	916.0	717.0
1975	801.8	811.1	646.0
1976	1009.5	1018.0	822.3
1977	884.3	882.1	684.8
1978	871.8	888.2	710.0
1979	1002.3	1012.2	859.9
1980	969.0	977.1	794.4
1981	1000.9	1006.7	832.0
1982	854.2	871.4	706.7
1983	980.6	998.7	833.7
1984	961.4	972.3	819.7
1985	874.3	882.3	706.2
1986	890.0	895.0	746.3
1987	991.6	993.4	769.8
1988	1160.8	1171.8	965.5
1989	942.0	955.0	777.8
1990	1026.1	1036.8	868.5
1991	949.2	963.0	796.6
1992	862.1	860.4	681.3
1993	688.1	681.2	489.1
1994	1011.8	1020.7	844.3
1995	812.9	811.1	649.8
1996	873.7	883.9	736.6
1997	957.6	967.3	819.7
1998	1112.1	1125.8	955.9
1999	855.8	857.4	640.7
2000	993.2	1008.1	815.5
2001	1148.6	1172.0	988.1
2002	814.0	829.7	711.3
2003	1091.5	1112.7	944.0
2004	837.1	844.0	637.7
2005	847.6	842.0	631.9
2006	1062.8	1085.2	944.1

Table B-4: Degree-day accumulations for Calgary, Alberta, from 1970 to 2006.

Year	Temporal sine method	Traditional sine method	Average method
1970	679.2	667.5	510.3
1971	670.2	656.5	475.1
1972	550.8	532.3	374.4
1973	575.7	559.2	407.5
1974	571.8	556.8	380.1
1975	558.3	542.6	366.1
1976	625.3	599.9	398.9
1977	552.1	489.3	289.9
1978	546.1	530.4	363.5
1979	646.5	621.4	332.1
1980	600.5	573.6	356.1
1981	611.6	597.7	416.2
1982	555.6	544.8	377.2
1983	652.6	640.9	472.3
1984	644.2	635.9	481.7
1985	581.4	561.6	391.9
1986	577.4	565.0	407.3
1987	698.3	675.2	447.2
1988	691.6	677.0	494.5
1989	596.4	583.0	418.7
1990	621.0	614.7	447.2
1991	619.5	606.1	431.7
1992	560.1	544.4	374.3
1993	438.2	413.6	239.3
1994	665.1	648.6	456.4
1995	491.1	478.3	316.0
1996	552.3	539.3	384.5
1997	601.7	587.5	410.5
1998	710.6	693.5	494.9
1999	503.3	484.8	292.9
2000	573.3	550.4	343.2
2001	690.5	670.0	483.9
2002	587.3	577.2	422.7
2003	707.9	699.9	527.4
2004	559.6	539.4	356.7
2005	499.2	484.9	285.0
2006	689.2	684.2	527.3

Table B-5: Degree-day accumulations for Edmonton, Alberta, from 1970 to 2006.

Year	Temporal sine method	Traditional sine method	Average method
1970	617.3	601.7	434.8
1971	585.2	567.2	386.4
1972	500.9	480.4	326.6
1973	512.5	498.9	351.8
1974	474.2	445.9	259.1
1975	490.4	463.3	253.9
1976	584.9	552.7	325.6
1977	493.6	455.3	220.3
1978	544.0	519.0	353.6
1979	546.5	529.2	360.9
1980	538.2	506.2	314.5
1981	632.9	610.4	426.1
1982	554.9	529.5	351.9
1983	581.2	561.2	400.0
1984	596.7	583.3	422.2
1985	533.2	573.6	410.3
1986	586.8	573.6	410.3
1987	599.7	576.1	371.6
1988	639.5	625.0	442.2
1989	572.9	560.9	403.1
1990	614.6	608.5	473.1
1991	633.8	620.7	459.7
1992	568.6	549.8	372.1
1993	501.5	471.2	290.3
1994	628.6	612.8	448.0
1995	490.0	479.0	316.4
1996	470.4	462.1	352.3
1997	609.1	609.2	498.8
1998	718.2	698.7	514.5
1999	506.4	481.2	302.5
2000	495.4	470.7	284.7
2001	596.4	566.9	351.8
2002	587.4	571.6	400.5
2003	632.1	606.5	422.6
2004	503.7	472.1	262.7
2005	480.7	451.3	258.8
2006	674.5	658.3	478.2

Table B-6: Degree-day accumulations for Saskatoon, Saskatchewan, from 1970 to 2006.

Year	Temporal sine method	Traditional sine method	Average method
1970	770.5	777.3	645.7
1971	735.1	730.0	574.9
1972	699.2	698.7	547.9
1973	717.1	719.7	582.5
1974	612.9	611.8	466.0
1975	665.7	664.3	502.9
1976	836.3	840.9	869.1
1977	686.0	680.9	514.6
1978	747.8	751.3	600.3
1979	764.8	777.5	648.1
1980	849.9	859.0	694.4
1981	882.9	889.0	750.7
1982	674.0	676.2	542.1
1983	805.4	825.9	700.2
1984	886.5	898.9	772.3
1985	623.9	620.2	483.8
1986	717.5	718.5	585.0
1987	834.6	835.1	644.6
1988	962.2	971.6	824.1
1989	800.1	809.6	679.2
1990	787.3	795.8	661.0
1991	863.4	876.3	749.0
1992	631.0	632.4	493.9
1993	551.7	536.2	356.6
1994	715.2	713.0	549.2
1995	681.7	673.1	516.8
1996	664.1	660.2	540.7
1997	791.1	794.5	646.3
1998	896.0	890.8	717.5
1999	633.0	628.0	459.7
2000	719.0	709.9	513.5
2001	927.9	925.3	739.0
2002	789.1	800.5	672.0
2003	928.5	928.6	762.7
2004	559.0	545.4	364.5
2005	603.4	590.5	422.8
2006	828.6	837.0	693.0

Table B-7: Degree-day accumulations for Estevan, Saskatchewan, from 1970 to 2006.

Year	Temporal sine method	Traditional sine method	Average method
1970	913.2	937.3	817.1
1971	860.4	863.3	699.3
1972	766.9	772.8	662.9
1973	892.3	906.4	762.1
1974	812.9	801.0	620.4
1975	793.7	805.3	675.6
1976	952.6	963.4	812.8
1977	905.8	902.1	734.5
1978	877.0	882.6	743.4
1979	858.2	878.3	746.7
1980	981.6	991.0	828.0
1981	-	-	-
1982	815.6	806.3	671.8
1983	1016.4	1037.5	887.7
1984	1029.8	1040.1	890.2
1985	769.1	777.1	620.8
1986	840.3	849.2	699.8
1987	1017.7	1026.5	848.7
1988	1214.7	1233.7	1068.1
1989	1006.4	1017.2	838.7
1990	890.7	899.3	739.1
1991	930.6	945.2	809.5
1992	710.8	707.7	509.4
1993	603.6	590.3	408.5
1994	803.5	801.0	634.7
1995	794.8	797.9	672.7
1996	764.6	772.4	645.9
1997	921.8	936.6	775.1
1998	942.3	951.2	779.2
1999	742.9	749.4	616.7
2000	803.4	800.5	616.5
2001	906.7	896.7	720.8
2002	803.1	809.7	684.6
2003	621.1	611.8	421.1
2004	820.1	827.5	664.1
2005	819.3	827.5	664.1
2006	945.8	946.2	775.1

Table B-8: Degree-day accumulations for Swift Current, Saskatchewan, from 1970 to 2006.

Year	Temporal sine method	Traditional sine method	Average method
1970	779.3	790.2	661.2
1971	788.0	788.6	627.4
1972	714.4	709.2	554.9
1973	789.7	786.4	619.8
1974	666.6	673.0	517.5
1975	645.1	643.2	490.0
1976	799.8	798.1	611.5
1977	684.8	675.6	483.2
1978	771.1	773.3	613.1
1979	774.2	785.5	653.2
1980	794.2	794.6	620.4
1981	784.5	787.1	615.9
1982	610.7	613.5	462.3
1983	812.4	825.1	672.8
1984	835.5	846.1	698.9
1985	674.6	674.6	514.3
1986	697.6	699.1	550.3
1987	789.7	788.8	590.7
1988	970.3	979.3	824.5
1989	729.5	732.7	592.5
1990	785.3	783.7	637.8
1991	788.5	794.1	637.8
1992	640.5	636.5	482.9
1993	539.9	523.0	342.9
1994	772.3	774.0	662.4
1995	-	-	-
1996	-	-	-
1997	-	-	-
1998	-	-	-
1999	-	-	-
2000	-	-	-
2001	-	-	-
2002	772.3	774.0	603.7
2003	925.9	941.8	791.2
2004	581.5	581.7	405.4
2005	684.7	678.6	520.9
2006	683.7	678.6	800.7

Table B-9: Degree-day accumulations for Dauphin, Manitoba, from 1970 to 2006.

Year	Temporal sine method	Traditional sine method	Average method
1970	800.6	815.3	694.7
1971	715.4	712.2	556.9
1972	709.3	699.3	552.3
1973	729.4	729.5	594.5
1974	674.1	670.7	542.5
1975	715.4	715.8	575.6
1976	843.8	843.4	688.7
1977	737.6	742.7	594.4
1978	739.7	742.7	594.4
1979	725.2	730.3	596.6
1980	835.7	840.8	685.7
1981	801.1	802.8	662.4
1982	699.3	698.5	547.2
1983	848.8	856.6	730.9
1984	828.9	833.2	690.2
1985	580.9	566.3	398.1
1986	717.6	710.5	558.2
1987	825.0	831.6	635.4
1988	944.9	952.4	831.0
1989	893.4	906.0	743.1
1990	759.0	757.0	631.7
1991	854.4	848.4	728.6
1992	561.3	546.5	395.1
1993	560.3	547.8	400.0
1994	-	-	-
1995	-	-	-
1996	559.9	547.8	591.1
1997	-	-	-
1998	844.2	847.5	700.6
1999	686.2	685.5	551.2
2000	703.0	700.7	529.0
2001	818.7	812.5	663.6
2002	818.3	812.5	684.1
2003	912.7	918.0	759.2
2004	554.2	548.8	394.0
2005	739.6	732.9	594.4
2006	740.0	732.9	738.8

Table B-10: Degree-day accumulations for Winnipeg, Manitoba, from 1970 to 2006.

Year	Temporal sine method	Traditional sine method	Average method
1970	881.4	899.6	796.2
1971	756.0	759.1	615.1
1972	835.4	849.1	699.8
1973	792.4	805.1	677.7
1974	769.9	784.4	663.0
1975	832.8	847.4	696.1
1976	947.7	966.4	824.9
1977	847.9	861.0	712.7
1978	859.7	869.8	740.6
1979	724.0	739.5	621.3
1980	952.6	977.4	834.9
1981	863.8	882.4	735.3
1982	769.6	783.6	634.5
1983	999.2	1007.8	903.4
1984	906.1	918.7	781.4
1985	681.3	983.6	531.8
1986	811.4	826.3	694.3
1987	970.8	988.9	835.0
1988	1132.4	1156.8	1031.9
1989	1003.7	1026.1	888.3
1990	918.4	939.8	827.1
1991	1013.9	1038.1	952.2
1992	623.1	623.2	504.7
1993	649.4	663.3	541.5
1994	799.3	806.6	677.0
1995	948.9	970.9	964.9
1996	822.1	845.3	742.8
1997	847.2	868.0	752.3
1998	926.5	931.9	784.6
1999	773.0	784.2	662.1
2000	784.9	789.2	613.5
2001	911.8	916.7	777.4
2002	870.6	889.7	785.6
2003	981.8	998.1	839.4
2004	608.0	607.2	466.8
2005	863.5	875.8	757.1
2006	1025.0	1046.2	912.6

Table B-11: Degree-day accumulations for Thompson, Manitoba, from 1970 to 2006.

Year	Temporal sine method	Traditional sine method	Average method
1970	459.4	453.4	394.3
1971	399.4	390.0	244.1
1972	437.2	426.2	292.1
1973	483.2	470.8	340.1
1974	395.2	388.7	296.3
1975	410.8	408.2	291.5
1976	517.0	512.9	367.6
1977	437.6	414.9	264.3
1978	291.1	283.1	165.7
1979	357.2	352.9	229.8
1980	427.9	415.6	244.8
1981	519.7	522.4	402.8
1982	375.3	371.0	241.7
1983	528.3	532.6	435.3
1984	546.8	550.0	437.9
1985	361.1	341.2	179.0
1986	396.3	395.6	265.8
1987	439.2	430.6	266.5
1988	548.0	543.2	407.0
1989	521.3	517.3	932.2
1990	486.4	478.4	321.1
1991	522.0	523.1	396.4
1992	338.0	323.1	180.5
1993	369.1	358.8	246.9
1994	473.6	463.7	304.1
1995	463.9	455.6	300.4
1996	508.5	506.8	366.2
1997	471.9	463.9	329.9
1998	551.8	544.5	397.1
1999	486.4	482.3	326.9
2000	421.5	416.6	283.7
2001	532.6	519.3	346.2
2002	469.7	467.6	351.9
2003	597.6	588.3	429.1
2004	344.8	330.2	194.3
2005	431.3	422.6	283.0
2006	525.9	516.2	368.2

Bibliography

[1] Allen, J. C. 1976. A modified sine wave method for calculating degree days. *Environmental Entomology*. 5: 388-396.

[2] Baskerville, G. L. and P. Emin. 1969. Rapid estimation of heat accumulation from maximum and minimum temperatures. *Ecology*. 50: 514-517.

[3] Berry, J. S., W. P. Kemp, J. A. Onsager. 1995. Within-year dynamics and forage destruction model for rangeland grasshoppers (Orthoptera: Acrididae). *Environmental Entomology*. 24(2): 212-225

[4] Broatch, J. S., L. M. Dosdall, G. W. Clayton, K. N. Harker, and R. Yang. 2006. Using degree-day and logistic models to predict emergence patterns and seasonal flights of the cabbage maggot and the seed corn maggot (Diptera: Anthomyiidae) in Canola. *Environmental Entomology*. 35: 1166-1177.

[5] Campbell, G. S., and J. M. Norman. *An Introduction to Environmental Biophysics* (Springer, New York, 1997).

[6] Church, N. S. and R. W. Salt. 1952. Some effects of temperature on development and diapause in eggs of *Melanoplus bivitattus* (Say) (Orthoptera: Acrididae). *Canadian Journal of Zoology*. 30: 173-184.

[7] Davidson, J. 1942. On the speed of development of insect eggs at constant temperatures. *Australian Journal of Experimental Biology and Medical Science*. 20: 233-239.

[8] Davidson, J. 1944. On the relationship between temperature and rate of development of insects at constant temperatures. *Journal of Animal Ecology*. 13: 26-38.

[9] Dennis, B., W. P. Kemp, and R. C. Beckwith. 1986. A stochastic model of insect phenology: estimation and testing. *Environmental Entomology*. 15: 540-546.

[10] Dennis, B., and W. P. Kemp. 1988. Further statistical inference methods for a stochastic model of insect phenology. *Environmental Entomology*. 17: 887-893.

[11] Eizenberg, H., J. Colquhon, and C. Mallory-Smith. 2005. A predicitve degree-day model for small broomrape (*Orobanche minor*) parasitism in red clover in Oregon. *Weed Science*. 53: 37-40.

[12] Eyring, H. 1935. The activated complex in chemical reactions. *Journal of Chemical Physics* 3: 107-115.

[13] FNA foods. (n.d). *Lentils*. Retrieved May 20th, 2011 from https://fnafoods.com/200910/lentils-15.html.

[14] Fisher, J. R. 1994. Temperature effect on post-diapause development and survival of embryos of three species of *Melanoplus* (Orthoptera: Acrididae). *Annals of the Entomological Society of America* 87: 604-608.

[15] Gage, S. H., M. K. Mukerji, and R. L. Randell. 1976. A predicti ve model for seasonal occurrence of three grasshopper species in Saskatchewan (Orthoptera: Acrididae). *Canadian Entomologist.* 108: 245-253.

[16] Gage, S. H., M. E. Whalon, and D. J. Miller. 1982. Pest event scheduling systems for biological monitoring and pest management. *Environmental Entomology* 11: 1127-1133.

[17] Government of Saskatchewan. 2006. *Saskatchewan Agriculture and Food Lentil.* Retrieved May 18th, 2011 from http://www.agriculture.gov.sk.ca.

[18] Governement of Saskatchewan. (n.d). Retrieved May 20th, 2011 from http://www.agriculture.gov.sk.ca/Default.aspx?DN=626d78ef-2444-4fae-98fc-95e05d88e759.

[19] Guppy J. C., and M. K. Mukerji. 1974. Effects of temperature on the immature stages of the alfalfa weevil, *Hypera postica* (Coleoptera:Chrysomelidae). *Canadian Entomologist.* 106: 93-100.

[20] Hewitt, G. B. 1979. Hatching and development of rangeland grasshoppers in relation to forage growth, temperature, and precipitation. *Environmental Entomology.* 8: 24-29.

[21] Higley, G. L., L. P. Pegido, and K. R. Ostlie. 1986. DEGDAY: A program for calculating degree-days, and assumptions behind the degree-day approach. *Environmental Entomology.* 15: 999-1018.

[22] Hilbert, D. W. 1995. Growth-based approach to modeling the development rate of arthropods. *Environmental Entomology.* 24: 771-778.

[23] Huffaker, C. B. 1944. The temperature relations of the immature stages of the malarial mosquito, *Anopheles quadrimaculatus* Say, with a comparison of the develomental power of constant and variable temperature in insect metabolism. *Annals of the Entomological Society of America.* 37: 1-27.

[24] Huffaker, C. B. and A. P. Gutierrez. *Ecological Entomology* (John Wiley and Sons Inc., New York, 1999).

[25] Hultin, E. 1955. The influence of temperature on the rate of enzymic process. *Acta Chemica Scandinavica.* 9: 1700-1710.

[26] *Insolation at specific locations* (n.d). Retrieved August 26, 2010 from http://aom.giss.nasa.gov/srlocat.html.

[27] Janisch, E. 1925. Über die Temperaturabhängigkeit biologischer Vorgange and ihre Kurvenmassige Analyse. *Pfluger's Archive. Ges. Physiol.* 209: 414-436.

[28] Janisch, E. 1932. The influence of temperature on the life-history of insects. *Transactions of the Royal Entomological Society of London.* 80: 137-168.

[29] Johnson, D.L. 2008. Grasshopper identification and control methods to protect crops and the environment. Published by the Saskatchewan Pulse Growers, and Agriculture and Agri-Food Canada, Pesticide Risk Reduction Program, Pest Management Centre, Ottawa. 42 pp.

[30] Johnson, D. L. 1989. Spatial autocorrelation, spatial modeling, and improvements in grasshopper survey methodology. *Canadian Entomologist.* 121: 579-588.

[31] Johnson, F. H., and L. Lewis. 1946. The growth rate of *E. coli* in relation to temperature, quinine and coenzyme. *Journal of Cellular and Comparative Physiology.* 28: 47-75.

[32] Kemp, W. P. and N. E. Sanchez. 1987. Differences in post-diapause thermal requirements for eggs of two rangeland grasshoppers. *Canadian Entomologist.* 119: 653-661.

[33] Kemp, W. P., T. M. Kalarik, and W. F. Quimby. 1989. Rangeland grasshopper (Orthoptera: Acrididae) spatial variability: Macroscale population assessment. *Environmental Entomology.* 82: 1270-1276.

[34] Kemp, W. P. and B. Dennis. 1989. Development of two rangeland grasshoppers at constant temperatures: Development thresholds revisited. *Canadian Entomologist.* 121: 363-371.

[35] Kemp, W. P. and B. Dennis. 1991. Toward a general model of rangeland grasshoppers (Othoptera: Acrididae) phenology in the steppe region of Montana. *Environmental Entomology.* 20: 1504-1515.

[36] Lactin, D. J., and D. L. Johnson. 1995. Temperature-dependent feeding of *Melanoplus sanguinipes* (Orthoptera: Acrididae) nymphs in laboratory trials. *Environmental Entomology* 24: 1291-1296.

[37] Lactin, D. J., N. J. Holliday, D. L. Johnson, and R. Craigen. 1995. Improved rate model of temperature-dependent development by arthropods. *Environmental Entomology.* 24(1): 68-79.

[38] Lactin, D. J., and D. L. Johnson. 1996. Behavioural optimization of body temperature by nymphal grasshoppers (*Melanoplus sanguinipes*, Orthoptera: Acrididae) in temperature gradients established using incandescent bulbs. *Journal of Thermal Biology.* 21: 231-238.

[39] Lactin, D. J., and D. L. Johnson. 1996. Effects of insolation and body orientation on internal thoracic temperature of nymphal *Melanoplus packardii* (Orthoptera: Acrididae). *Environmental Entomology.* 25: 423-429.

[40] Lactin, D. J., and D. L. Johnson. 1998. Environmental, physical, and behavioural determinants of body temperature in grasshopper nymphs (Orthoperta: Acrididae). *Canadian Entomologist.* 130: 551-577.

[41] Lactin, D. J., and D. L. Johnson. 1998. Convective heat loss and change in body temperature of grasshoppers and locust nymphs: Relative importance of wind speed, insect size and insect orientation. *Journal of Thermal Biology.* 23: 5-13.

[42] Lamb, J. R., and S. R. Laschiavo. 1981. Diet, temperature, and the logistic model of developmental rate for *Tribolium confusum* (Coleoptera: Tenebrionidae). *Canadian Entomologist.* 113: 813-818.

[43] Lockwood, J. A. and D. R. Lockwood. 1991. Rangeland grasshoppers (Orthoptera: Acrididae) population dynamics: insights from catastrophe theory. *Environmental Entomology.* 20(4): 970-980.

[44] Logan, J. A., D. J. Wollkind, S. C. Hoyt, and L. K. Tanigoshi. 1976. An analytic model for description of temperature development rate phenomena in arthrodpods. *Environmental Entomology.* 5: 1133-1140.

[45] Logan, J. A. 1988. Toward an expert system for development of pest simulation models. *Environmental Entomology.* 17: 350-376.

[46] Lysyk T. J. 2007. Seasonal abundance, parity, and survival ofadult *Culicoides sonorensis* (Diptera: Ceratopogonidae) in Southern Alberta, Canada. *Journal of Medical Entomology* 44(6): 959-969.

[47] Matthews, J. H. *Numerical Methods for Mathematics, Science and Engineering.* (Prentice Hall, Eaglewood Cliff, New Jersey, 1992).

[48] Messenger, P. S., and N. E. Flitters. 1958. Effect of constant temperature environments on the egg stage of three species of Hawaiian fruit flies. *Annals of the Entomological Society America.* 51: 109-119.

[49] Motulsky, H. J., and L. A. Ransas. 1987. Fitting curves to data using nonlinear regression: a practical and nonmathematical review.*The Journal of the Federation of American Societies of Experimental Biology.* 1: 365-374.

[50] Mukerji, M. J., S. H. Gage, and R. L. Randell. 1976. A quantitative evaluation of grasshopper (Orthoptera: Acrididae) damage and its effects on spring wheat. *Canadian Entomologist.* 108: 255-270.

[51] Mukerji, M. J., S. H. Gage, and R. L. Randell. 1977. Influence of embryonic development and heat on population trend of three grasshopper species in Saskatchewan (Othoptera: Acrididae). *Canadian Entomologist.* 109: 229-36.

[52] Nelder, J. A., and R. Mead. 1965. A simplex method for function minimization. *Computer Journal.* 7: 308-313.

[53] *Nelder-Mead algorithm.* 2009. Retrieved July 15, 2010 from http://www.scholarpedia.org/article/Nelder-Mead-algorithm.

[54] Onsager, J. A., and W. P. Kemp. 1986. Rangeland grasshoppers (Orthoptera: Acrididae) modeling phenology of natural populations of six species. *Environmental Entomology.* 15: 924-930.

[55] Onsager, J. A. 2000. Action window for optimum control of rangeland grasshoppers (Orthoptera: Acrididae). *J. Economic Entomology.* 98: 308-314.

[56] Olfert, O. and A Slinkard. 1999. Grasshopper (Orthoptera: Acrididae) damage to flowers and pods of lentil *Lens culinaris L. Crop Protection.* 18: 527-530.

[57] Olsson, D. M. and L. S. Nelson. 1975. The Nelder-Mead simplex procedure for function minimization. *Technometrics* 17: 45-51.

[58] Pannell, D. J. 1991. Pests and pesticides, risk and risk aversion. *Agricultural Economics.* 5: 361-383.

[59] Price, C. J., I. D. Coope, D. Byatt. 2002. A convergent variant of the Nelder-Mead algortihm. *Journal of Optimization Theory and Applications.* 113: 5-19.

[60] Pruess, K. 1983. Day-degree methods for pest management. *Environmental Entomology.* 12: 613-619.

[61] Quednav, W. 1957. Über den Einfluss von Temperatur und Luftfeuchtigkeit auf den Eiparasiten *Trichogramma cacoeciae* Marchal. Mitt. Biol. *Bundesanstalt Land Forstwirtsch. Berlin* 90: 1-63.

[62] Quinn, M. A., R. L. Kepner, D. D. Wagenbach, R. N. Foster, R. A. Bohls, P. D. Pooler, K. C. Reuter, and J. L. Swain. 1993. Grasshopper stages of development as indicators of nontarget athropod activity: Implications for grasshopper programs on mixed-grass rangeland. *Environmental Entomology.* 22: 532-540.

[63] Randell, R. L. and M. K. Mukerji. 1974. A technique for estimating hatching of natural egg populations of *Melanoplus sanguinipes* (Orthoptera: Acrididae). *Canadian Entomologist.* 106: 801-812.

[64] Rathjen, W. 1939. Experimentelle untersuchugen zur Biologie und Ökologie von *enoicyla pusilla* Burm. *Z. Morph. Oekol. Tiere.* 35: 14-83.

[65] Riegert, P. W. 1968. A history of grasshopper abundance surveys and forecasts of outbreaks in Saskatchewan. *Memoirs of the Entomological Society of Canada*. 52: 5-12.

[66] Richards, F. J. 1959. A flexible growth function for empirical use. *Journal of Experimental Botany*. 10: 290-300.

[67] Schoolfield, R. M., P. J. H. Sharpe, and C. E. Magnuson. 1981. Nonlinear regression of biological temperature-dependent rate models based on absolute reaction-rate theory. *Journal of Theoretical Biology*. 88: 719-731.

[68] Sharpe, P. J. H., and D. W. DeMichele. 1977. Reaction kinetics of poikilotherm development. *Journal of Theoretical Biology*. 64: 649-670.

[69] Sharpe, P. J. H., G. L. Curry, D. W. Demichele, and C. L. Cole. 1977. Distribution model of organism development times. *Journal of Theoretical Biology*. 66: 21-38.

[70] Singer, S and Sanja Singer. 2004. Efficient implementation of the Nelder-Mead search algorithm. *Applied Numerical Analysis and Computational Mathematics*. 1: 524-534.

[71] Smith, D. S. and N. D. Holmes. 1977. The distribution and abundance of grasshoppers (Acrididae) in crops in Alberta, 1918-1975. *Canadian Entomologist*. 109: 575-592.

[72] Spendley, W., G. R. Hext, and F.R. Himsworth. 1962. Sequential application of simplex designs in optimisation and evolutionary operation. *Technometrics*. 4: 441-446.

[73] Statistics Canada. 2009, *Seeding Intentions Survey*. Retrieved May 20th, 2011 from http://www.agriculture.gov.sk.ca/SeedingIntentions2009

[74] Stinner, R. E., A. P. Gutierrez, and G. D. Butler, Jr. 1974. An algorithm for temperature-dependent growth rate simulation. *Canadian Entomologist*. 106: 519-524.

[75] Taylor, R. G., and D.G. Harcourt. 1978. Effect of temperature on development rates of the immature stages of *Crioceris asparagi* (Cleoptera: Chrysomelidae).*Canadian Entomologist*. 110: 57-62.

[76] *Telescoping sums*. (n.d). Retrieved June 5, 2010 from http://planetmath.org/encyclopedia/Telescope.html.

[77] Thomas, P. A. 1980. Life-cycle studies on *Paulinia acuminata* (DeGreer) (Othoptera: Paulinniidae) with the particular reference to the effects of constant temperature. *Bulletin Entomological Research*. 70: 381-389.

105

[78] *Types of insect metamorphosis* (n.d) Retrieved July 12, 2010 from http://insects.about.com/od/growthmetamorphosis1.

[79] University of California. 2003. *Degree-days*. Retrieved May 15, 2010 from http://www.ipm.ucdavis.edu/WEATHER/ddconcepts.html.

[80] Utah State University. (n.d). *Using degree-day treatments for insect pests*. Retrieved Feb. 8th, 2011 from http://climate.usurf,usu.edu/includes/pestFactSheets/degree-days08.pdf.

[81] Verhulst, Pierre-François. 1838. Notice sur la loi que la population poursuit dans son accroissement. *Correspondance mathématique et physique.* 10: 113-121.

[82] Vickery, V. R. 1979. Notes on some Canadian Acrididae (Orthoptera). *Canadian Entomologist.* 111: 699-702.

[83] Wagner, T. L., H. Wu, P. J. H. Sharpe, R. M. Schoolfield, and R. N. Coulson. 1984. Modeling insect development rates: A literature review and application of a biophysical model. *Annals of the Entomological Society America.* 77: 208-225.

[84] M. Goodwin. Pulse Canada. Personal communication.

[85] D. Johnson. Personal communication 1.

[86] D. Johnson. Personal communication 2.